universität wien

DIPLOMARBEIT / DIPLOMA THESIS

Titel der Diplomarbeit / Title of the Diploma Thesis

„Antiproliferative effect of TRPV1 ligands in vascular smooth muscle cells: is it TRPV1 dependent?"

verfasst von / submitted by

Hannah Cäcilia Mathis

angestrebter akademischer Grad / in partial fulfilment of the requirements for the degree of

Magistra der Pharmazie (Mag.pharm.)

Wien, 2021/ Vienna, 2021

Studienkennzahl lt. Studienblatt / degree programme code as it appears on the student record sheet:	A 449
Studienrichtung lt. Studienblatt / degree programme as it appears on the student record sheet:	Diplomstudium Pharmazie
Betreut von / Supervisor:	Univ.-Prof. Dr. Verena Dirsch
Mitbetreut von / Co-Supervisor:	Dr. Tina Blazevic

Table of Contents

List of Abbreviations

APS	Ammonium persulfate
BrdU	Bromo-deoxyuridine
BSA	Bovine serum albumin
cDNA	Complementary DNA
CDK	Cyclin-dependent kinase
CKI	Cyclin-dependent kinase inhibitor
CRISPR	Clustered regularly interspaced short palindromic repeats
CVD	Cardiovascular disease
DCB	Drug -coated balloon
ddH_2O	Double-distilled water
DES	Drug-eluting stent
DMEM	Dulbecco's Modified Eagle Medium
DMSO	Dimethyl sulfoxide
DNA	Deoxyribonucleic acid
EC	Endothelial cell
ECL	Enhanced chemiluminescence
EDTA	Ethylenediaminetetraacetic acid
FACS	Fluorescence activated cell sorting
FBS	Fetal bovine serum
HAM's F-12	F-12 Nutrient Mixture
HFS	Hypotonic fluorochrome solution
HRP	Horseradish peroxidase
HS	Horse serum
INT	Iodonitrotetrazolium
KO	Knockout

LDH	Lactate dehydrogenase
mRNA	Messenger RNA
NAD^+	Nicotinamide adenine dinucleotide
NGF	Nerve growth factor
PAA	Polyacrylic acid
PAGE	Polyacrylamide gel electrophoresis
PBS	Phosphate-buffered saline
PCI	Percutaneous coronary intervention
PCR	Polymerase chain reaction
PDGF	Platelet-derived growth factor
PI	Propidium iodide
PMSF	Phenylmethylsulfonyl fluoride
PVDF	Polyvinylidene fluoride
RB	Retinoblastoma protein
RIPA	Radioimmunoprecipitation assay buffer
RNA	Ribonucleic acid
RPMI	Roswell Park Memorial Institute
RT	Reverse transcriptase
RT-qPCR	Real time quantitative polymerase chain reaction
SDS	Sodium dodecyl sulfate
TEMED	Tetramethylethylenediamine
TBS-T	Tris-buffered saline with Tween
TRPV	Transient receptor potential vanilloid
VSMC	Vascular smooth muscle cell
WT	Wild type

1. Abstract

Atherosclerosis, an inflammatory disease, causes narrowing of blood vessels and leads to heart attack and stroke. It is one of the most common causes of death worldwide. Therapy of advanced atherosclerosis often includes stent implantation. However, the disadvantage of this procedure is a mechanism called in-stent restenosis. Aberrant proliferation of vascular smooth muscle cells (VSMC) leads to this re-narrowing of the blood vessels. Inhibition of VSMC therefore is an important target regarding the prevention of atherosclerosis.

In this study, we examined the effect of the TRPV1 ligands piperine, capsaicin, evodiamine, capsazepine, SB-366791 and BCTC on the proliferation of VSMC.

This diploma thesis reveals the anti-proliferative effect of evodiamine in VSMC. The anti-proliferative effect is due to a G2/M arrest of PDGF-induced VSMC upon evodiamine treatment. Previous findings from the study group could corroborate this result.

In addition, we could detect TRPV1 mRNA in VSMC. However, we cannot state that TRPV1 is indeed expressed in our VSMC model. Antibodies used for western blot seem to bind rather unspecific and may not be able to detect TRPV1.

1.1. Zusammenfassung

Atherosklerose, eine entzündliche Erkrankung, führt zu einer Verengung der Blutgefäße und zu Herzinfarkt und Schlaganfall. Es ist eine der häufigsten Todesursachen der Welt. Die Therapie der fortgeschrittenen Atherosklerose umfasst häufig eine Stentimplantation. Der Nachteil dieses Verfahrens ist jedoch ein Mechanismus, der als In-Stent Restenose bezeichnet wird. Übermäßige Proliferation von glatten Gefäßmuskelzellen (VSMC) führt zu dieser erneuten Verengung der Blutgefäße. Die Proliferationshemmung der VSMC ist daher ein wichtiges Ziel bei der Prävention der Atherosklerose.

In dieser Studie untersuchen wir den Effekt von TRPV1 Liganden wie Piperin, Capsaicin, Evodiamin, Capsazepin, SB-366791 und BCTC auf die Proliferation von VSMC.

Diese Diplomarbeit zeigt den antiproliferativen Effekt von Evodiamine in VSMC. Die antiproliferative Wirkung beruht auf einem G2/M Arrest von PDGF-induzierten VSMC nach Behandlung mit Evodiamine. Frühere Ergebnisse aus der Studiengruppe konnten dieses Ergebnis bestätigen.

Zusätzlich konnten wir TRPV1 mRNA in VSMC nachweisen. Jedoch können wir nicht sagen, dass TRPV1 in unserem VSMC Modell exprimiert wird. Die Antikörper, die hierfür verwendet wurden, binden vielmehr unspezifisch und können TRPV1 vielleicht nicht detektieren.

2. Introduction

2.1. Atherosclerosis

Atherosclerosis is a disease affecting the large arteries and therefore often leading to heart disease and stroke. It is responsible for approximately 50% of all deaths in the western world. A healthy blood vessel consists of three different layers. The innermost layer, the intima, is composed of endothelial cells and elastic fibers. The middle layer, called media, is made of smooth muscle cells and the outer layer, the adventitia, consists of connective tissues (Figure 1)[1].

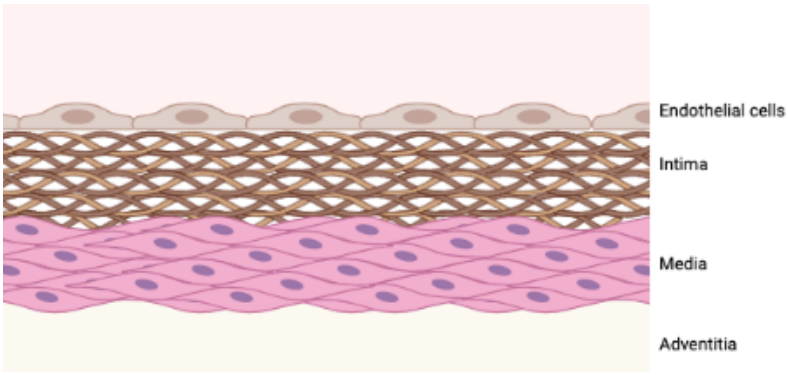

Figure 1: Structure of a healthy artery. *Adopted from Lusis A.J.*[1]

2.1.1. Pathogenesis

Focal thickenings of the intima are called atherosclerotic lesions. Development of these lesions results from early changes in the endothelium leading to endothelial dysfunction. Endothelial cells (EC) express intracellular adhesion molecules as well as vascular cell adhesion molecules, which bind to monocytes. After adhesion to the EC and stimulation through chemokines, monocytes migrate to the intima and become macrophages. The macrophages take up oxidized LDL particles leading to the formation of foam cells. EC also release cytokines and growth factors, which stimulate VSMC proliferation and migration to the intima. Foam cells, lipid-laden monocytes and T-lymphocytes build the initial fatty streaks. Later on, these fatty streaks also include VSMC[2].

Different atherogenic factors (diabetes, hypertension, smoking, LDL cholesterol) can cause endothelial dysfunction and initiate the release of cytokines and growth factors. As a response, VSMC start to migrate, proliferate and assemble extracellular matrix components. This leads to formation

of a firm fibrous cap, contributing to the stability of the plaque. However, VSMC are also responsible for thinning and rupture of the fibrous cap. Inflammatory mediators lead to expression of proteases and ultimately apoptosis of VSMC[3].

Risk factors for atherosclerosis include smoking, hypertension, diabetes mellitus, hyperlipidemia as well as male gender, age and genetic disposition[4].

2.1.2. Therapy

It is important that atherosclerosis is detected early on. Therapy begins with lifestyle changes, these include reducing risk factors: quit smoking, losing weight, exercise, reduce stress and consume a low-fat diet. When these lifestyle measures are not successful in reducing the overall cardiovascular risk, medical therapy can be included: HMG-CoA-reductase inhibitors are used to reduce high levels of LDL, antiplatelet drugs lead to an extenuated aggregation of thrombocytes[5].

If blood flow is already limited, operative measures such as percutaneous transluminal angioplasty, intracoronary stents or coronary artery bypass surgery are used to help restore blood flow[6]. Due to high rates of restenosis after angioplasty, stents can be implanted to keep the vessels open and prevent restenosis. Although bare metal stents have advantages over angioplasty, those stents lead to high rates of in-stent restenosis. To prevent in-stent restenosis, drug-eluting stents (DES) have been developed. DES include anti-proliferative drugs such as paclitaxel or sirolimus. These anti-proliferative drugs are able to reduce VSMC proliferation and therefore decrease the high risk of in-stent restenosis. However, compared to bare metal stents, first generation drug-eluting stents (paclitaxel, sirolimus) result in a higher risk of late stent thrombosis. This risk can be reduced when using second generation drug-eluting stents like cobalt chromium everolimus-eluting stents[7]. DES contain a polymeric coating, which is responsible for carrying and releasing the anti-proliferative drug. However, it may also be responsible for an inflammatory response occurring in the vascular wall[8].

Drug-coated balloons (DCB) are also an important tool for the treatment of in-stent restenosis. Compared to drug eluting stents, DCB have the advantage that there is no permanent scaffold[9].

2.1.3. Restenosis

If blood flow in stenotic vessels is compromised, percutaneous intervention (PCI) and coronary bypass surgery are common therapeutic options. Those approaches often lead to increased narrowing of blood vessels, namely restenosis[10].

If restenosis occurs in an implanted stent, it is called in-stent restenosis. Vascular injury, developed during PCI or stent implantation, leads to a complex inflammatory response. Additionally, platelet-derived growth factors cause VSMC to proliferate and migrate from the media to the intima resulting in extracellular matrix formation[8].

Drug-eluting stents have reduced the incidents of neointimal proliferation, which plays an important role in the development of in-stent restenosis.

2.2. Vascular smooth muscle cells

Vascular smooth muscle cells are located in the middle layer of blood vessels, called media. They are important elements in common vascular repair and also pathologic processes. In healthy blood vessels they respond to normal stimuli with vasoconstriction and dilatation. VSMC are also responsible for the synthesis of collagen, elastin and the release of growth factors and cytokines. Upon vascular injury, such as loss of endothelial cells or endothelial dysfunction, VSMC proliferate and migrate from the media to the intima and begin to form what is called the neointima. However, excessive healing response leads to intimal thickening, which may cause stenosis of small or medium blood vessels[11].

VSMC are able to change their phenotype from a contractile to a synthetic type. Contractile VSMC are located in healthy vessels and express high levels of contractile proteins. Phenotypically switched (de-differentiated) VSMC, or the synthetic type, produce higher levels of extracellular matrix[12].

VSMC engage in the development of atherosclerosis: they produce extracellular matrix and, in response to PDGF, migrate from the media to the intima leading to narrowing and wall thickening[13].

2.3. Cell cycle

Quiescent cells respond to extracellular stimulation and move from the G0 phase to the G1 phase, in which they are preparing for the following synthesis (S) phase. After successful DNA replication, cells go through another gap phase (G2), in order to prepare for the following mitosis (M) phase. The M phase includes separation of cellular components and division of the cell into two separate cells[14] (Figure 2).

Regulation of the cell cycle is mainly ensured by cyclin-dependent kinases (CDK). In addition, further controlling of the cell cycle is guaranteed through cell cycle checkpoints, making sure DNA replication and other critical events are completed properly[14].

As seen in Figure 2, the first checkpoint is located at the end of the G1 phase. If cell size is adequate and there is no DNA damage, the cell cycle will presume throughout the S-phase. The second checkpoint, at the end of the G2 phase, verifies that DNA replication has been completed properly and at the end of the M phase, the last checkpoint ensures that the chromosome set is correct[15].

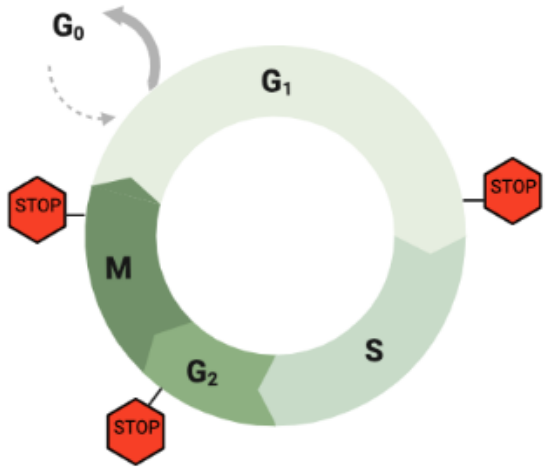

Figure 2: Cell cycle of a eucaryotic cell. *G0 phase (quiescent cells), G1 phase (gap 1), S phase (synthesis), G2 phase (gap 2) and M phase (mitosis). Control of the cell cycle is ensured through 3 checkpoints (stop signs). After W. Müller-Esterl[15]*

In order for their activation, cyclin-dependent kinases need to be associated with a cyclin subunit[16]. In mammalians, 9 cyclin-dependent kinases (CDK 1-9) have been detected so far. Additionally, there are several mammalian cyclins. A few of these CDKs and cyclins also function outside of the cell cycle and are responsible for DNA repair, apoptosis or regulation of transcription[17]. All eucaryotic cells are provided with cyclins. Together with their associated CDKs, cyclins fulfil their functions in different

phases of the cell cycle[18]. The first cyclins which are induced as soon as G0 cells enter the cell cycle are the D-type cyclins (D1, D2, D3). Levels of D-type cyclins are regulated by the presence of growth factors. D-type cyclin kinases have one main substrate, namely the retinoblastoma protein (RB)[17].

The retinoblastoma (RB) pathway is important for the first restriction point. Retinoblastoma proteins are able to bind numerous members of the E2F family, which are responsible for entry and progression through the S-phase. Expression of E2F target genes is negatively regulated by binding through retinoblastoma proteins. Phosphorylation of the retinoblastoma protein by CDKs leads to transcription of target genes and therefore stimulates progression into S-phase[19].

The activity of cyclin-dependent kinases is also affected by cyclin-dependent kinase inhibitors (CKI). CKIs are small proteins which are able to inhibit cyclin-CDK complexes. There are two families of CKIs: INK4 proteins and CIP/KIP proteins. INK4 proteins bind to either CDK4 or CDK 6 and therefore inhibit activation of those two CDKs. CIP/KIP proteins are able to inhibit several of the CDKs. Both families of CKIs are capable of preventing cell cycle progression and thus act as tumor suppressors[18].

2.4. TRPV1 channel

The TRPV1 channel belongs to a class of cation channels named transient receptor potential channels. Originally the channels were identified in *Drosophila*, where deletion of the *trp* gene left only a transient response compared to a sustained depolarization in the presence of light. However, mammalian TRP channels are important for communication. They react to several stimuli and in return allow the entry of cations. Activation of TRP channels in neurons leads to depolarization, in non-excitable cells they are involved in regulating intracellular calcium concentrations and therefore also responsible for relaxation and proliferation of cells[20].

The TRP superfamily is further divided into six subfamilies, namely TRPC (Canonical), TRPM (Melastatin), TRPA (Ankyrin), TRPML (Mucolipin), TRPP (Polycystic) and TRPV (Vanilloid). They are able to alter membrane potential or intracellular calcium concentration[21].

TRP channels are homotetramers, each one consisting of six transmembrane segments (Figure 3). The S1-S4 domain, the S4-S5 linker, as well as the TRP domain may be involved in ligand binding. There is also an N-terminal domain and a C-terminal domain facing the cytosol. The ion filter is formed by the S5-S6 domain and is permeable for Ca^{2+} and Na^{+} (Figure 4)[22].

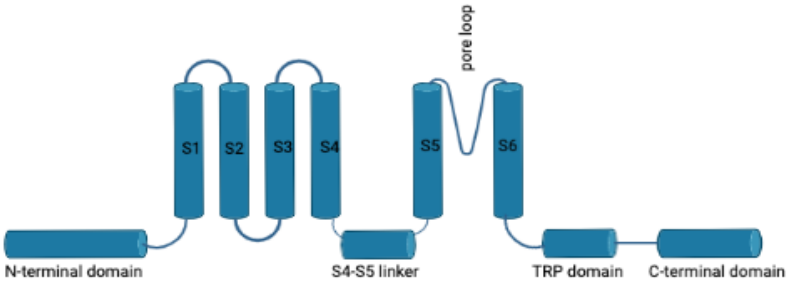

Figure 3: Structure of TRP channels. *They consist of six transmembrane segments. The S5-S6 domain is forming a pore loop permeable for ions. Adopted from Zhang et al.*[22]

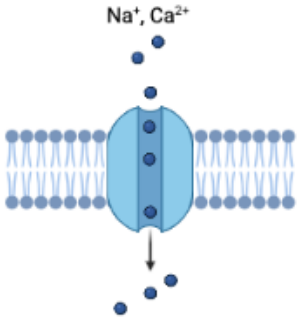

Figure 4: Permeability of the TRP channels*. The ion filter is permeable for* Ca^{2+} *and* Na^{+}*. Adopted from Zhang et al.*[22]

The TRPV (transient receptor potential vanilloid) channels were named after capsaicin, a vanilloid like molecule, component of hot chili peppers and activator of this TRPV subfamily. TRPV1 is also activated by high temperatures (>42°C) and low pH. Ligand binding is usually followed by a painful feeling and burning sensation, making the TRPV1 channels interesting therapeutic targets regarding pain medication[21,23].

So far reports on the TRPV1 expression in VSMC have been inconsistent. Studies have shown that TRPV1 is expressed in arteriolar smooth muscle cells. Activation of TRPV1 here leads to an increased intracellular Ca^{2+} concentration as well as vasoconstriction. Results of functional measurements were contradicting. Some arteries responded to capsaicin with constriction, others had a very limited functional response to capsaicin. This could be due to the existence of different splice variants of TRPV1[23]. Other studies have shown that TRPV1 is located in the vascular endothelium and that TRPV1 agonists lead to dilation of blood vessels and therefore decrease blood pressure[24].

2.4.1. TRPV1 ligands

2.4.1.1. TRPV1 agonists

Figure 3 shows the structure of all TRPV1 agonists used in this study. Evodiamine is an indole alkaloid and natural component of *Evodiae fructus*. It is associated with anti-nociceptive, anti-inflammatory and anti-neoplastic effects. Therefore, *Evodiae fructus* is traditionally used in China for treating different kinds of pain, such as headaches and abdominal pain[25]. Studies have shown that evodiamine acts as a TRPV1 agonist. Due to the structural differences compared to capsaicin, evodiamine could function as a potential new lead for the development of TRPV1 agonists[26].

The TRPV1 agonist piperine is an alkaloid and major constituent in the fruits of *Piper nigrum* L.. It is commonly used as a spice due to its pungency. Traditionally, *Piper nigrum* L. is used to relieve pain[27]. Piperine also functions as an anti-oxidative and anti-inflammatory substance. Studies suggest that piperine inhibits PDGF-sinduced VSMC proliferation, therefore also leading to an anti-proliferative effect[28].

The TRPV1 agonist capsaicin is a natural alkaloid component of the fruits of *Capsicum frutescens* L.. It is responsible for the pungent flavor of chili peppers[29]. Capsaicin has various effects such as anti-inflammatory, thermogenic and analgesic. Topical applications of capsaicin are widely used to reduce pain[30].

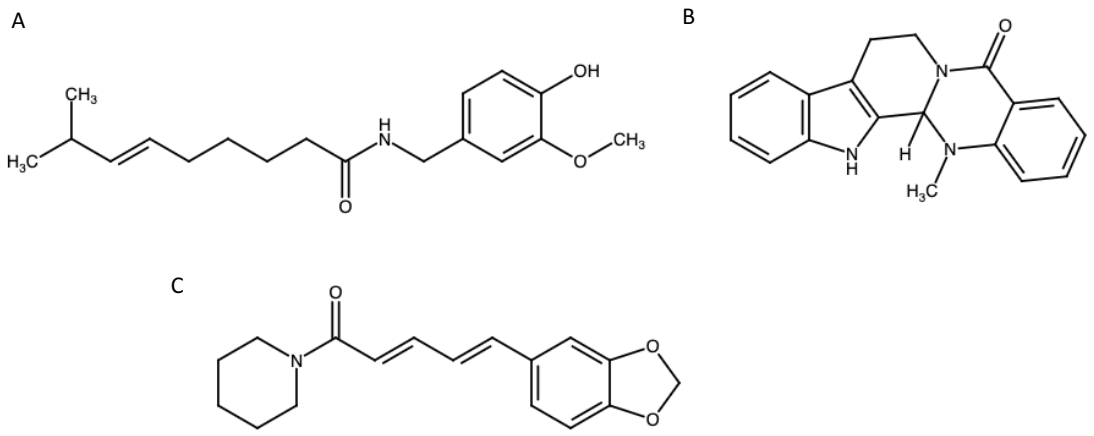

Figure 3: Structure of the TRPV1 agonists used. *Capsaicin (A), evodiamine (B) and piperine (C).*

2.4.1.2. TRPV1 antagonists

All TRPV1 antagonists used in this study are shown in Figure 4. Capsazepine is a TRPV1 antagonist and blocks responses to the TRPV1 agonist capsaicin[31]. It is a synthetic analogue of capsaicin and acts as competitive antagonist[32]. BCTC is, like capsazepine, a TRPV1 antagonist[33]. Both of these antagonists are rather non-selective and have also shown inhibition of TRPM8[34]. A more selective and potent, cinnamide TRPV1 antagonist is SB-366791. It is commonly used in pain research[35,36].

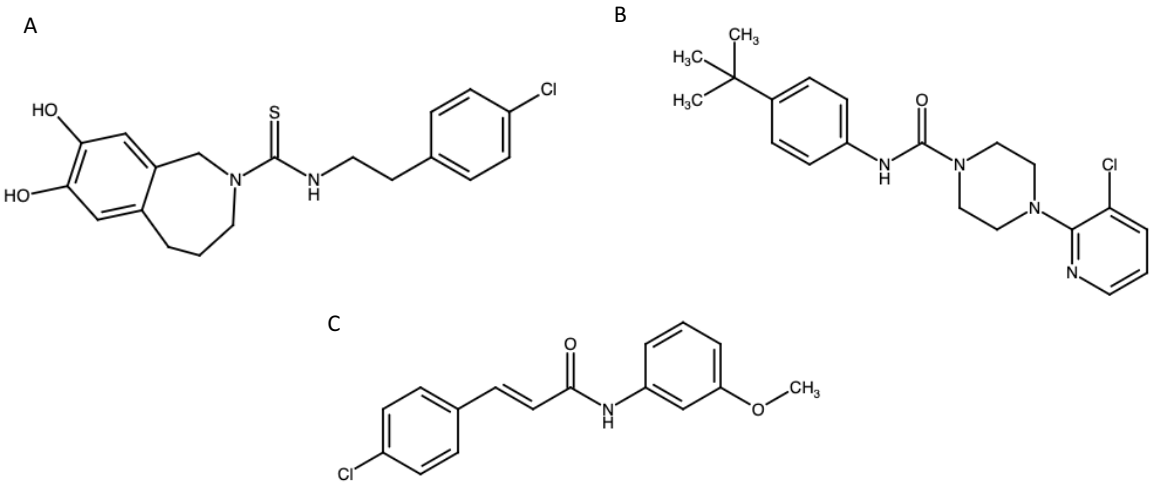

Figure 4: Structure of the TRPV1 antagonists used. *Capsazepine (A), BCTC (B) and SB-366791 (C).*

2.5. PDGF

Platelet-derived growth factors act as potent mitogens for several cell types including fibroblasts and smooth muscle cells. The PDGF family consists of four different polypeptide chains which are encoded by four different genes. Through homo- or heterodimerization the chains form into disulfide-linked dimers, leading to five dimeric isoforms: PDGF-AA, PDGF-AB, PDGF-BB, PDGF-CC and PDGF-DD[37].

PDGF receptors are tyrosine kinase receptors. Ligand binding results in receptor dimerization, activation of intrinsic receptor tyrosine kinase and phosphorylation of receptor molecules[38].

A substantial role in the proliferation of vascular smooth muscle cells plays PDGF[39]. The expression of all PDGF isoforms in atherosclerotic lesions compared to healthy vessels is increased. PDGF therefore is a crucial factor in the progression of vascular diseases. Various immune cells secrete PDGF upon activation, leading to VSMC proliferation and migration into the intima. Several treatments, such as inhibition of the PDGF pathway as well as neutralizing PDGF antibodies, can lead to reduction of the VSMC accumulation in atherosclerosis[40].

3. Aim of the Work

Atherosclerosis leads to serious consequences like myocardial infarction, stroke or peripheral artery disease and therefore has a huge impact on human health worldwide[41]. As previously discussed (2.1.3), VSMC migration from the media to the intima and aberrant VSMC proliferation leads to in-stent restenosis. Thus, inhibiting VSMC proliferation is an important goal in preventing in-stent restenosis.

Previous research from the "Molecular targets" group has shown that TRPV1 ligands, such as evodiamine, inhibit the proliferation of VSMC.

The aim of this diploma thesis is to investigate the possible anti-proliferative effect of various other TRPV1 ligands and additionally to determine whether the effect is TRPV1 dependent with the special focus on the TRPV1 expression in our VSMC model.

4. Results

4.1. Cytotoxicity of TRPV1 ligands in VSMC

To exclude that any anti-proliferative effect of TRPV1 ligands is caused by cytotoxicity, LDH release assay was previously performed in our study group with the TRPV1 ligands evodiamine and capsaicin. In this study we also worked with the TRPV1 ligands piperine, capsazepine, SB-366791 and BCTC, therefore the LDH release assay was additionally performed for those substances.

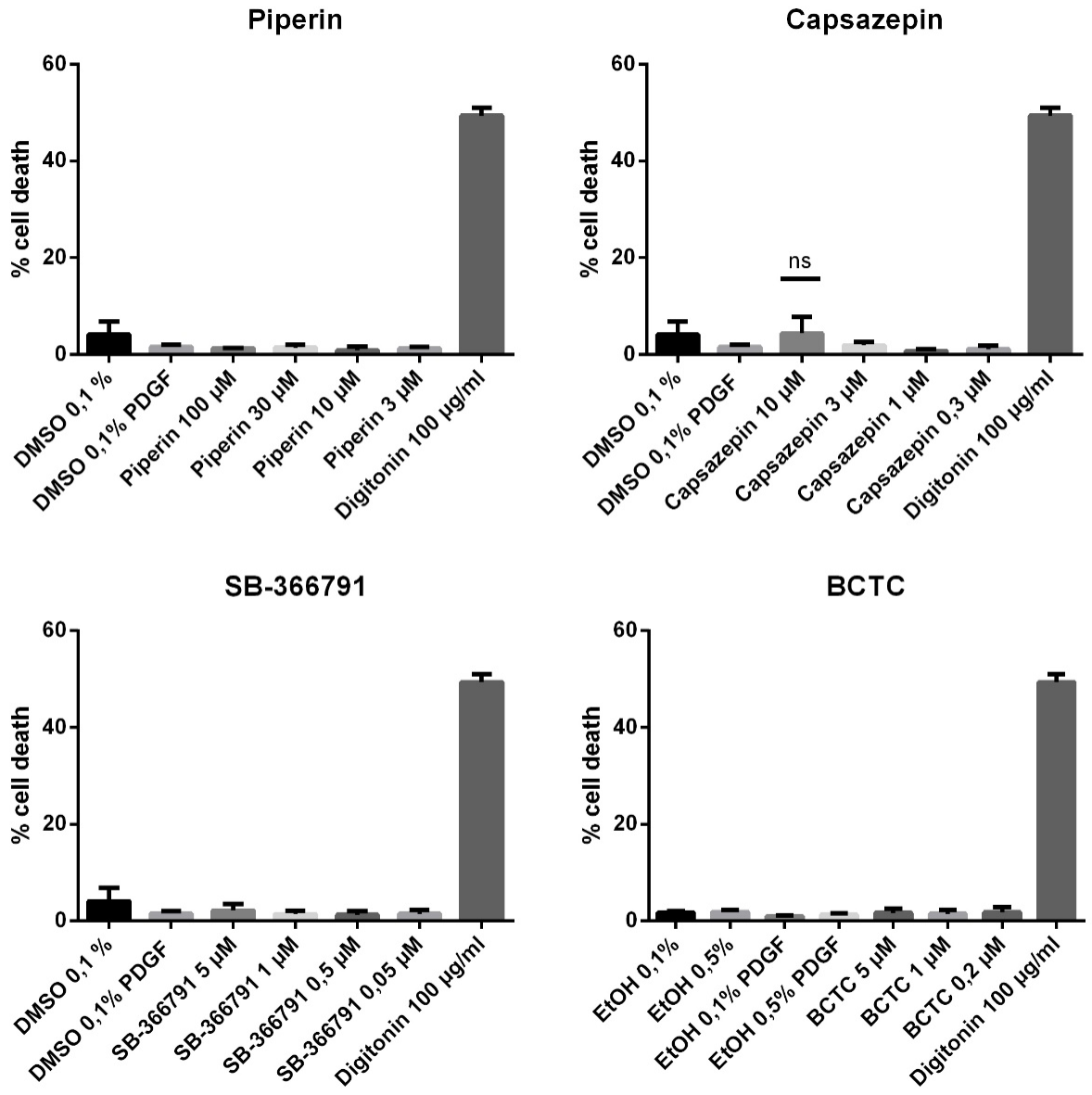

Figure 5: Compounds as seen above are not cytotoxic in VSMC. *VSMC were treated with compounds, vehicle or digitonin for 30 min, as indicated, then stimulated with PDGF for 24 h. (Mean ± SD, n=3, ns not significant, ANOVA).*

VSMC were treated with different concentrations of the TRPV1 ligands piperine, capsazepine, SB-366791 and BCTC or vehicle for 30 min and then stimulated with PDGF for 24 h.

Compared to the positive control digitonin, above mentioned compounds could not increase the LDH release and are not cytotoxic within the tested concentration range in VSMC (Figure 5).

4.2. G2/M arrest of evodiamine

BrdU and resazurin data from the study group have shown that cells stop proliferating when treated with capsaicin and piperine. Nuclear PI staining was performed to assess in which cell cycle phase cells get arrested.

VSMC were treated with compounds or vehicle, stimulated with PDGF and then analyzed using flow cytometry.

After 16 h of treatment all cells find themselves in the G2/M phase. Capsaicin and capsazepine treated cells seem to progress slower through cell cycle, as they accumulate in the S phase at 16 h time point. There are significantly more cells treated with 30 μM and 3 μM capsaicin in the S phase compared to the DMSO PDGF control. As for evodiamine, there are less cells in the G0/G1 phase and more cells in the G2/M phase compared to the DMSO PDGF control (Figure 7).

After 24 h a significant amount of the evodiamine treated cells are still in the G2/M phase. There are significantly less cells in the G0/G1 phase compared to the DMSO PDGF control. Similar to evodiamine, a significant amount of cells treated with 30 μM capsaicin are in the G2/M phase. In comparison to the DMSO PDGF control, almost the same amount of cells are in the G0/G1 phase. As for SB-366791 and BCTC, there are significantly more cells in the G0/G1 phase and less in the S phase (Figure 8).

These results lead to the conclusion that evodiamine is causing cell cycle arrest. Capsaicin and capsazepine only seem to slow down cell cycle progression and piperine does not seem to interfere with the cell cycle progression at all.

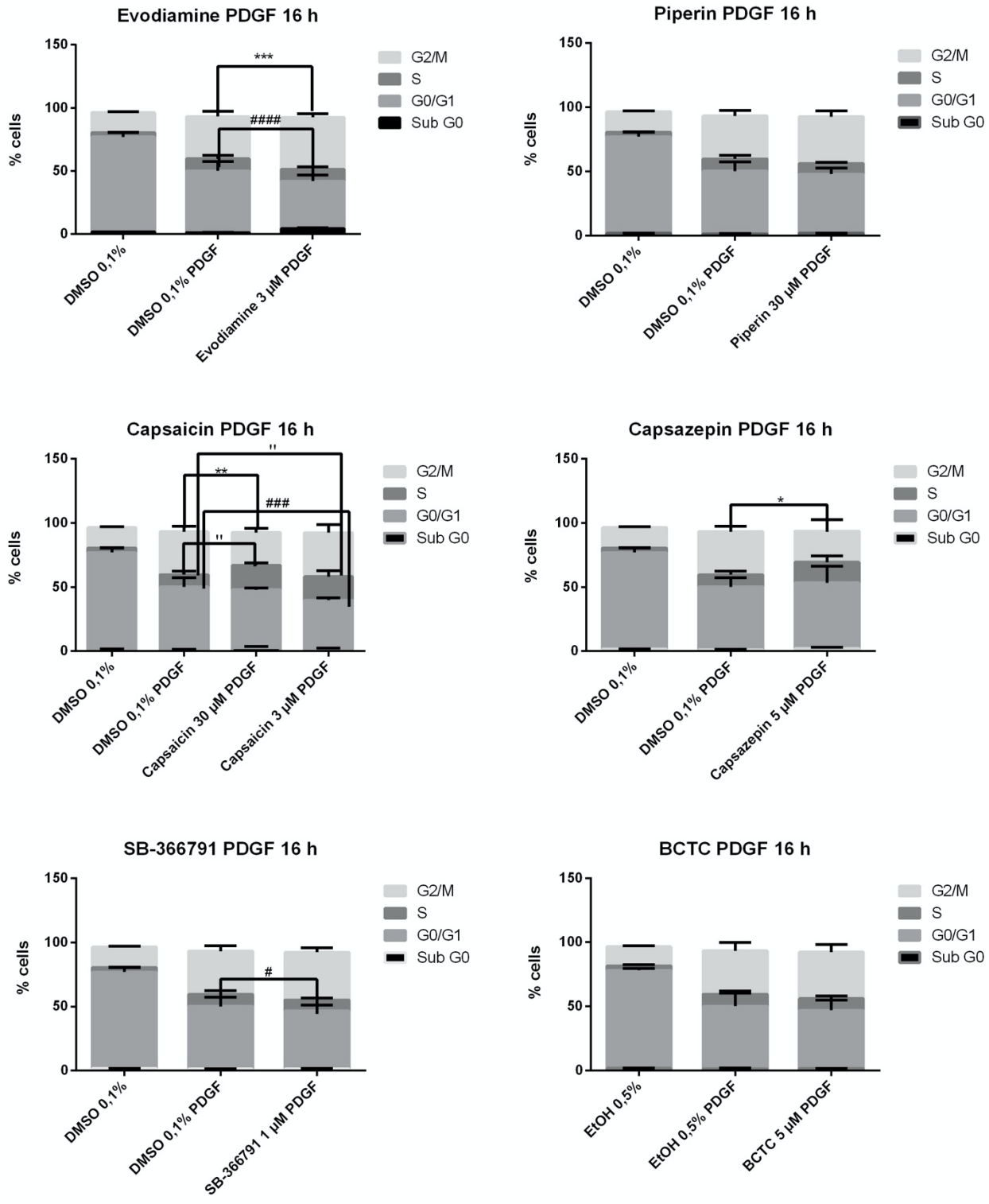

Figure 7: ***TRPV1 ligands and PDGF-induced cell cycle progression at 16 h.*** *VSMC were treated with compounds or vehicle for 30 minutes, as indicated, then stimulated with PDGF for 16 h. Cell cycle analysis was performed via PI staining of nuclei and flow cytometry. n=3, ' S, # G0/G1, * G2/M (* p < 0.5, ** p < 0.01, *** p < 0.001, **** p < 0,0001, ANOVA).*

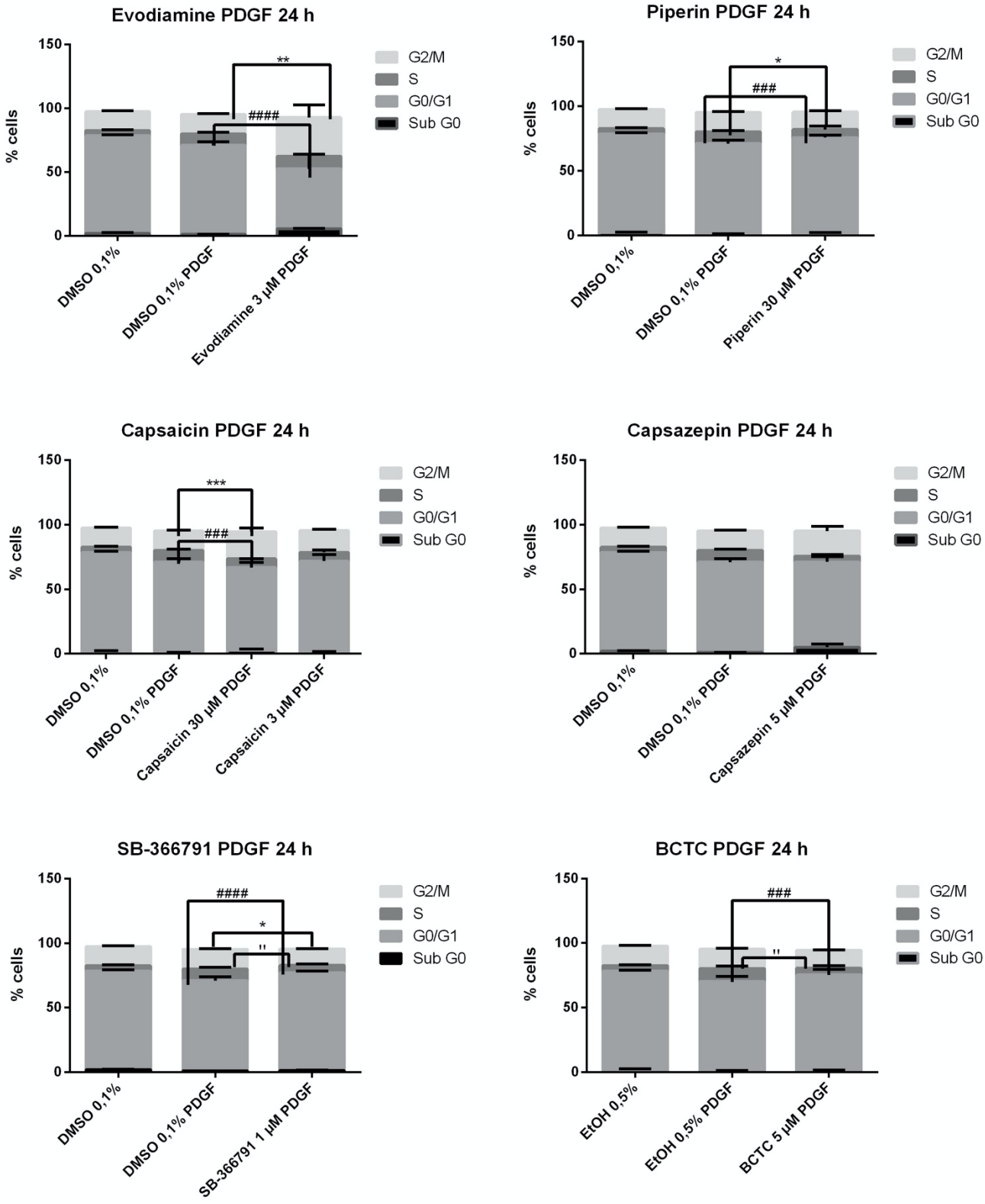

Figure 8: TRPV1 ligands and PDGF-induced cell cycle progression at 24 h *VSMC were treated with compounds or vehicle for 30 minutes, as indicated, then stimulated with PDGF for 24 h. Cell cycle analysis was performed via PI staining of nuclei and flow cytometry. n=3, ´S, # G0/G1, * G2/M (* p < 0.5, ** p < 0.01, *** p < 0.001, **** p < 0.0001, ANOVA).*

4.2.1. Co-treatment with TRPV1 antagonists overrides the G2/M arrest of evodiamine

As previously shown, evodiamine treated cells get arrested in the G2/M phase (Figure 8). Former experiments from the study group indicated that the TRPV1 antagonists capsazepine and SB-366791 override the G2/M arrest of evodiamine in VSMC. Co-treatment of evodiamine with those antagonists was therefore performed to ensure the reproducibility of this effect. Here we used antagonists in concentrations that do not interfere greatly with the cell cycle progression in VSMC, as observed in Figure 7 and Figure 8.

Cells were treated with 3 µM evodiamine alone and co-treated with 3 µM evodiamine + 5 µM capsazepine and 3 µM evodiamine + 1 µM SB-366791. PDGF was used to stimulate cells after 16 h and 24 h, respectively. 0.1% DMSO PDGF was used as control.

After 16 h almost half of the evodiamine treated cells were in the G2/M phase. Co-treatment of evodiamine and capsazepine, as well as co-treatment of evodiamine and SB-366791, abolished the effect of evodiamine, as there are less cells in the G2/M phase (Figure 9). The effect of co-treatment of evodiamine and capsazepine is significantly different from the monotreatment. Although the effect of co-treatment of evodiamine and SB-366791 is not significant, there is a trend showing less cells in the G2/M phase in co-treated cells than in monotreated cells.

Compared to the DMSO PDGF control, co-treated cells seem to remain stuck at the beginning in the G0/G1 phase. There are less cells in the G2/M phase and more in the G0/G1 phase.

After 24 h PDGF-stimulated cells should be in the G0/G1 phase again. Evodiamine treated cells are arrested in the G2/M phase, however this effect is abolished when cells are co-treated with evodiamine and capsazepine and also evodiamine and SB-366791 (Figure 10), suggesting a potential TRPV1 dependency in the evodiamine related inhibition of VSMC proliferation. Additionally, the number of cells treated with evodiamine and co-treated with antagonists increased in the sub G0 phase, indicating that they are quiescent and not proliferating.

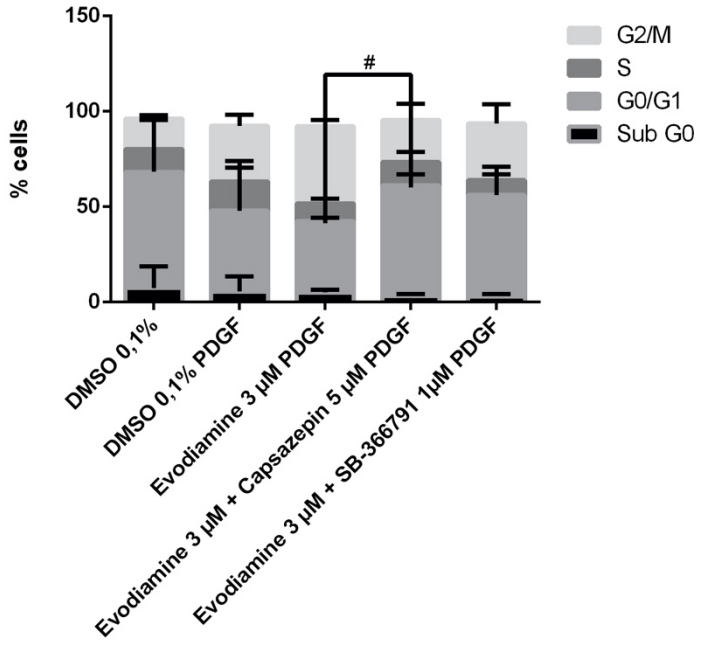

Figure 9: TRPV1 antagonists override the G2/M phase arrest caused by evodiamine after 16 h. *VSMC were treated with compounds or vehicle for 30 minutes, as indicated, then stimulated with PDGF for 16 h. Cell cycle analysis was performed via PI staining and flow cytometry. n=4, # G0/G1 (* p < 0.05, ANOVA).*

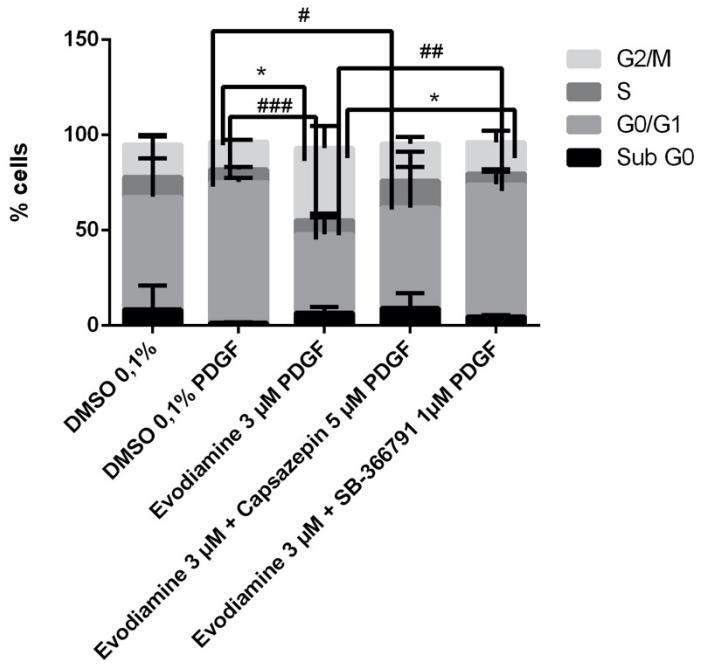

Figure 10: TRPV1 antagonists override the G2/M arrest caused by evodiamine after 24 h. *VSMC were treated with compounds or vehicle for 30 minutes, as indicated, then stimulated with PDGF for 24 h. Cell cycle analysis was performed via PI staining and flow cytometry. n=4, # G0/G1, * G2/M (* p < 0.05, ** p < 0.01, *** p < 0,001, ANOVA).*

4.3. Trypan blue exclusion

Former results from the study group using BrdU assay and Resazurin assay indicate that cells stop growing when treated with TRPV1 ligands. However, cell cycle progression was not inhibited when VSMC were treated with piperine, SB366791 and BCTC. Due to these conflicting data, we wanted to examine how the treatment with TRPV1 ligands reflects on the absolute cell number of viable cells (and viability) using the trypan blue exclusion approach and the Vi-Cell™ cell counter machine.

Here as well, VSMC were treated with compounds for 30 min, then stimulated with PDGF for 24 h .

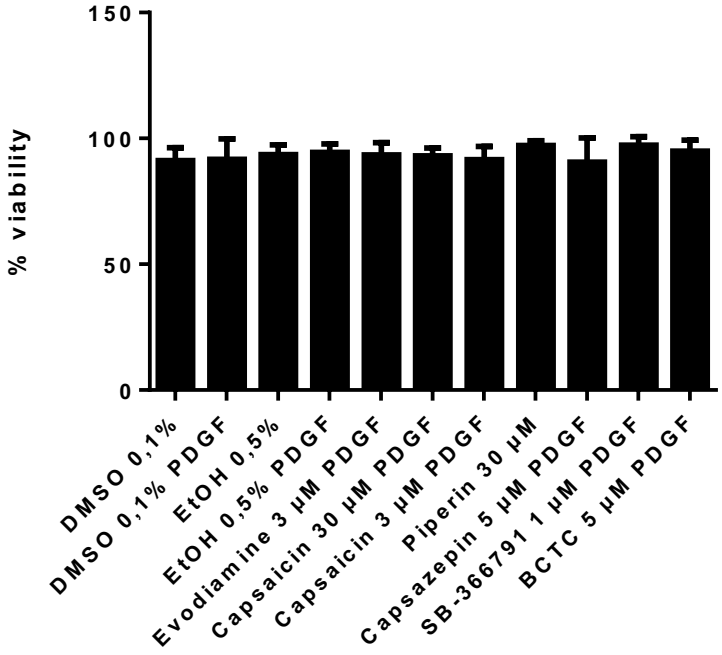

Figure 11: Viability of VSMC treated with TRPV1 ligands. *VSMC were treated with compounds or vehicle for 30 min, as indicated, then stimulated with PDGF for 24 h. % viability was calculated by ViCell cell counter as an average partition of trypan blue excluding cells (live cells) within the whole cell population counted out of 50 obtained images. n=3*

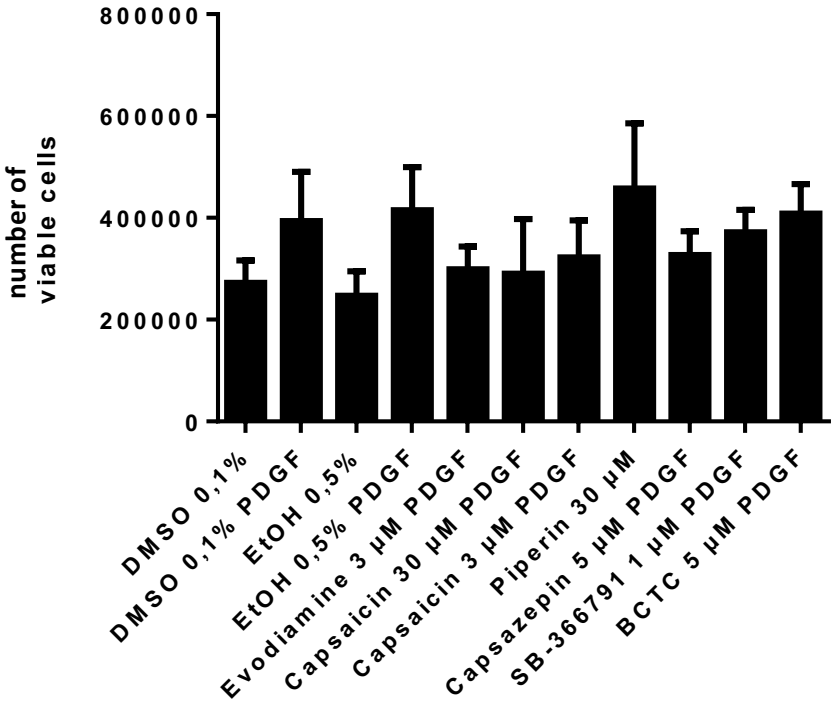

Figure 12: Viable cells*. VSMC were treated with compounds or vehicle for 30 min, as indicated, then stimulated with PDGF for 24 h. n=3. The number of live cells was calculated by multiplying the total volume of the cell suspension with the number of cells per ml of cell suspension. The latter was extrapolated based on the number of living cells counted in 50 obtained images in the ViCell cell counter machine.*

Viability from all treatments is as good as with the DMSO PDGF/EtOH PDGF control (Figure 11).

The results also show that with evodiamine (3 µM), capsaicin (3 µM and 30 µM) and capsazepine (5 µM) there are less cells counted than in the DMSO PDGF control (Figure 12). Compared to the PDGF controls there is a similar amount of viable cells for piperine (30 µM), SB-366791 (1 µM) and BCTC (5 µM). In concentrations shown to be sufficient to inhibit the BrdU incorporation and resazurin conversion, piperine, SB-366791 and BCTC did not reduce the overall VSMC number in trypan blue exclusion test. Together with the observed uninterrupted cell cycle progression in the presence of these compounds in PDGF-stimulated VSMC (Figure 7 and Figure 8), we conclude that these three TRPV1 ligands do not act anti-proliferative in VSMC, at least not at these specific concentrations.

4.4. TRPV1 expression in VSMC

Reports on the TRPV1 expression in VSMC have been inconsistent so far. Western blot studies were therefore performed to investigate if TRPV1 is actually present in our VSMC model. Two different commercially available antibodies against TRPV1 were used: 1) rabbit polyclonal against the N-terminal end and 2) mouse monoclonal against the C-terminal end. TRPV1 expression was examined in VSMC, A-10 WT cells and four different strains of A-10 TRPV1 KO cells. PC12 cells, undifferentiated and differentiated, were used as positive controls for TRPV1 expression. α,β-Tubulin was used as loading control.

The TRPV1 band was expected at approximately 100 kDa size.

All three experiments showed a strong band at 120 kDa and an additional strong band at around 47 kDa with the mouse monoclonal antibody. Using the rabbit polyclonal antibody, a strong band is seen at 110 kDa and 210 kDa (Figure 13).

Furthermore, there are two weaker bands in the differentiated PC-12 cells at around 90 kDa in experiment 1 and 2 with the mouse monoclonal antibody (Figure 13A, B).

Although A-10 TRPV1 KO cells should not express TRPV1, bands are seen with both antibodies used in all three experiments, some of them even stronger than in the A-10 WT cells (Figure 13). Thus, I would not conclude that these antibodies are good and specific in detecting TRPV1. Even if the used antibodies are unspecific, our VSMC model could still express TRPV1.

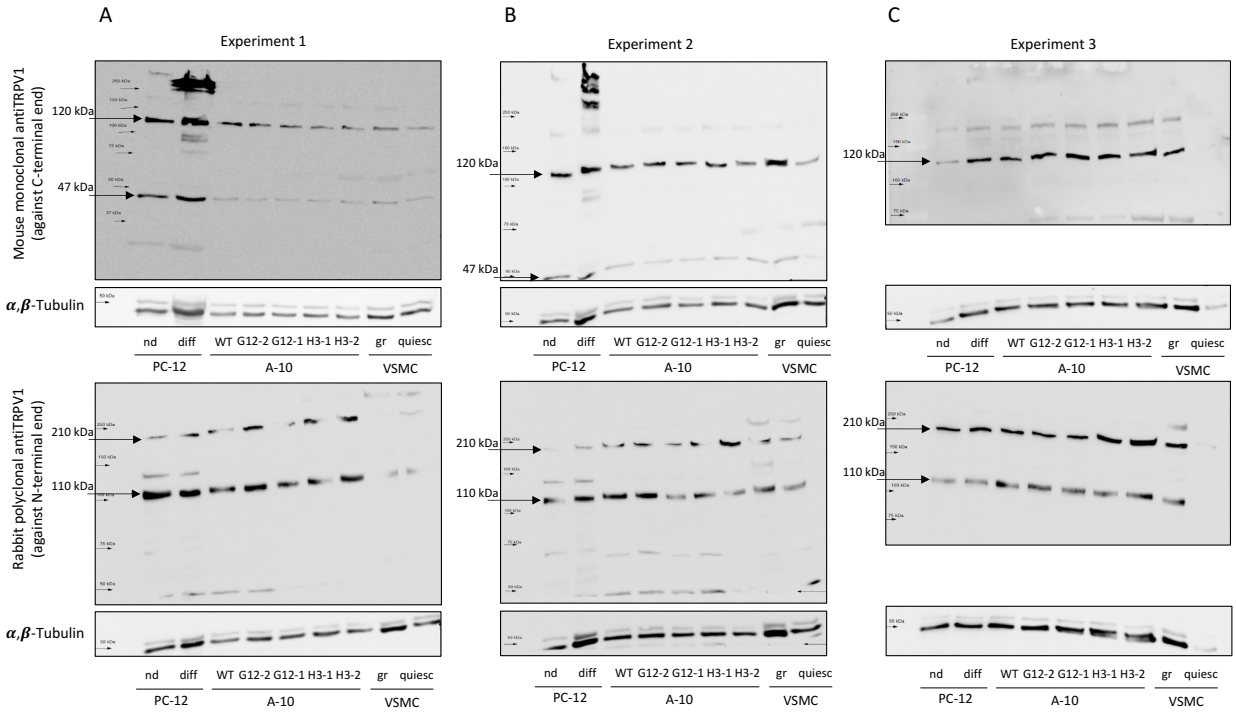

Figure 13: Detection of TRPV1 expression using western blot. *VSMC were grown for two days (gr) or serum deprived (quiesc) for the last 24 h of the 2-day period. A-10 WT (WT) and A-10 TRPV1 KO (G12-2, G12-1, H3-1, H3-2) cells were grown for two days. PC-12 cells were grown for two days (nd) or differentiated with 100 ng/ml NGF for 11 days (diff). Blots shown are from three independent experiments.*

4.5. TRPV1 mRNA expression in VSMC

Since the results from the western blot studies were inconclusive, we decided to examine the TRPV1 mRNA expression in our VSMC model using RT-qPCR. Three different custom designed primers (Table 12) for rat TRPV1 were used and tested in differentiated and undifferentiated PC-12 cells. Undifferentiated PC-12 cells do not seem to express TRPV1 mRNA, as the melting curves for all three primers were not good, which indicates multiple PCR products, and the signal for TRPV1 appeared at the same cycle as those from negative controls: water, RT+ (with reverse transcriptase) and RT- (without reverse transcriptase) samples. Only the primer set 1 produced a nice signal in differentiated cells and the melting curve showed only one peak, suggesting that differentiated PC-12 cells do express the mRNA for TRPV1.

Two experiments with VSMC were performed, one set of VSMC grown in culture medium and another one with VSMC serum deprived for 24 h, to mimic the experimental setup in proliferation assays. Results here show that, as before, only the primer set 1 produced a nice signal and one melting curve. However, the signal for TRPV1 appeared at a much later cycle than the signal for GAPDH, which was

diluted 20 times, whereas TRPV1 was undiluted. This suggests that our VSMC does not express a lot of TRPV1 mRNA.

In the first experiment, serum deprived VSMC (D1) expressed somewhat more TRPV1 mRNA than VSMC grown for 2 days. Results from the second experiment showed an even higher increase of TRPV1 mRNA in serum deprived VSMC (D2) compared to the VSMC grown for two days (Figure 14).

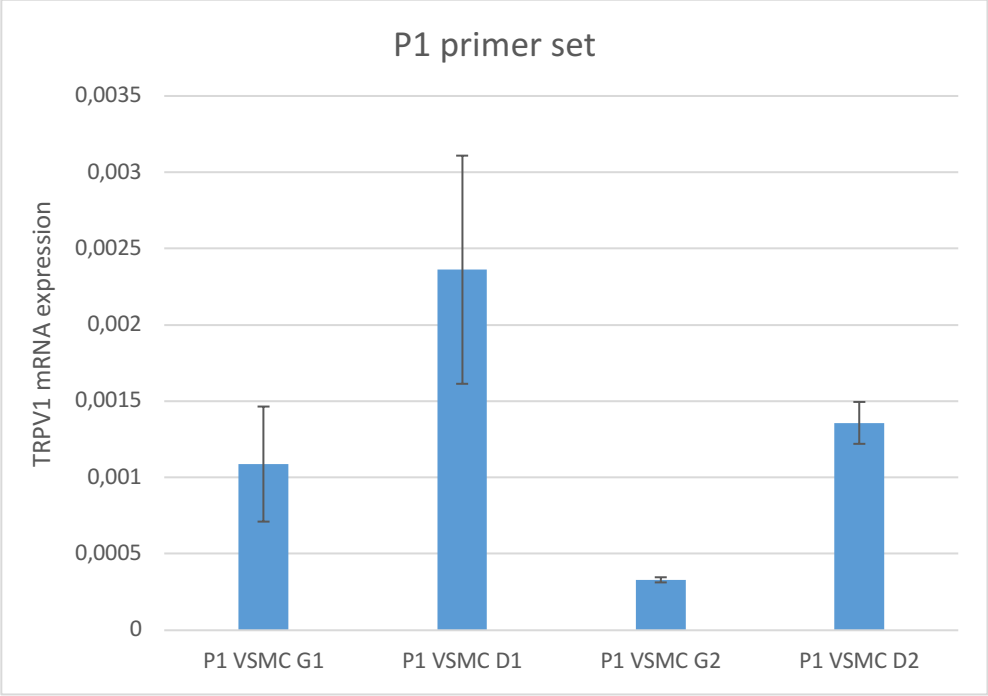

Figure 14: VSMC express TRPV1 mRNA. *VSMC were grown for 2 days (G) or serum-deprived (D) for the last 24 h of the 2-day period. Cells were lysed and RNA isolated using the PeqGOLD Total RNA Kit. cDNA was synthesized using the Applied Biosystems™ High Capacity cDNA Reverse Transcription Kit. RT-qPCR was performed using the Luna® Universal qPCR Master Mix measuring all samples in triplicates. GAPDH was used as loading control. Graph shows results normalized to loading control, using the primer set 1 (P1) for both experiments, 1 and 2,.*

4.6. Phalloidin staining of VSMC

Former results from the study group of phalloidin staining showed rearrangement of the actin cytoskeleton upon evodiamine exposure. Here, we performed two more experiments to further examine the reproducibility of this effect and whether TRPV1 might play a role in this effect.

VSMC were seeded onto gelatin-coated coverslips and treated with vehicle or evodiamine. Fixed cells were then stained with phalloidin and Hoechst and observed using a confocal microscope.

In all experiments performed, we could not reproduce the effect of evodiamine on the actin cytoskeleton. Exposure to evodiamine for 6 h did not lead to substantial changes in actin cytoskeleton rearrangement (Figure 15).

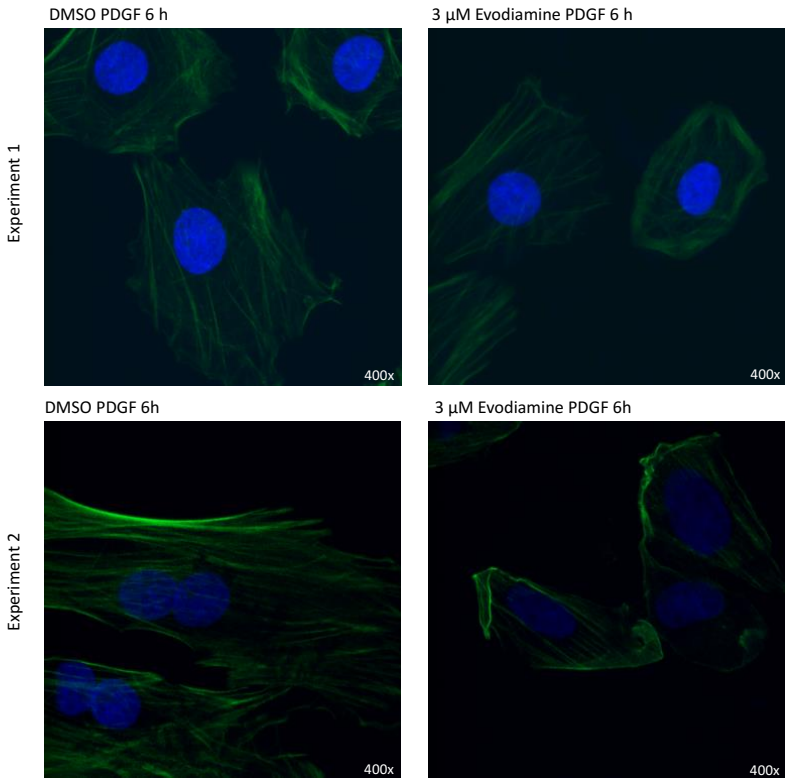

Figure 15: Phalloidin staining of VSMC. Evodiamine does not affect actin cytoskeleton. *VSMC were treated with 0.1% DMSO or 3 µM Evodiamine for 30 minutes, then stimulated with PDGF for 6 h. Fixed cells were stained with phalloidin (green) and Hoechst (blue) and observed using a confocal microscope.*

5. Discussion

5.1. Antiproliferative effect of evodiamine

Out of all six TRPV1 ligands tested in this study, evodiamine, capsaicin and capsazepine are the only compounds with an anti-proliferative effect in VSMC. Trypan blue exclusion showed that, compared to the DMSO PDGF control, cells treated with evodiamine, capsaicin and capsazepine stop growing (Figure 12). As the results from the LDH assay show, this effect is not due to cytotoxicity of the compounds used (Figure 5).

Previous results from the study group using BrdU and Resazurin conversion assay also show that evodiamine and capsaicin inhibit PDGF-induced VSMC proliferation. However, these results also indicated that cells stop growing after being treated with piperine. These different observations could be due to the fact that all three assays are based on various principles.

The resazurin conversion assay is based on the conversion of resazurin to resorufin in proliferating cells. This process is dependent on enzymatic conversion[42,43]. Nonenzymatic redox reactions in the presence of our tested compounds could be the reason for false results. BrdU (5-bromo-2'-deoxyuridine) is an analog of thymidine. During the S-phase of the cell cycle it is incorporated into the DNA of proliferating cells[44]. Since the S-phase is slowed down in capsaicin and capsazepine treated cells, this might explain why these cells incorporated less BrdU.

5.2. Cell cycle arrest of evodiamine

Cells, which get arrested in certain phases of the cell cycle stop proliferating. Nuclear PI staining of PDGF-induced VSMC revealed a G2/M arrest of evodiamine treated cells after 24 h (Figure 8). Apart from capsazepine (slower progression through the S-phase), TRPV1 antagonists did not affect cell cycle progression. However, compared to evodiamine alone, a significant increase in the percentage of cells in the G0/G1 phase was observed in evodiamine treated cells that were co-treated with either capsazepine or SB-366791 after 16 h and 24 h PDGF stimulation (Figure 9, Figure 10).

The fact that the TRPV1 antagonists are able to override the anti-proliferative effect of evodiamine, suggests a possible TRPV1 dependency in the evodiamine related inhibition of VSMC. Studies have

previously shown that capsaicin inhibits proliferation of human urinary bladder cells and that this effect is overridden by capsazepine and SB-367791, therefore also suggesting a TRPV1 dependency[45].

Capsaicin and capsazepine treated cells seem to accumulate in the S-phase at 16 h time point, but since they find themselves in the G0/G1 phase again after 24 h it does not look like they inhibit VSMC proliferation, but rather slow it down. Since the S-phase is slowed down, this might explain why capsaicin and capsazepine-treated VSMC incorporated less BrdU in the respective proliferation assay. Even though there is a significant amount of 30 μM capsaicin treated cells still in the G2/M phase after 24 h, this effect is absent in 3 μM capsaicin treated cells. In the trypan blue exclusion, the number of cells decreased after capsaicin treatment. This leads to the conclusion that capsaicin and capsazepine can ameliorate the overall proliferation of PDGF-induced VSMC, by slowing down the S-phase.

As mentioned above, cells treated with a higher concentration of capsaicin showed a small significant effect after 24 h, whereas a lower concentration did not show any effect. Potentially, the anti-proliferative effect of capsaicin could occur in a concentration-dependent manner and the concentrations used in our PI staining were too low.

5.3. TRPV1 expression in VSMC

Results with the rabbit polyclonal antibody showed strong bands at around 110 kDa and also at around 210 kDa in all three experiments performed. With the mouse monoclonal antibody, there are strong bands at around 120 kDa and weaker ones at around 47 kDa.

Concerning the A-10 cells, we could observe bands in both the WT and KO cells at around 100 kDa in all three experiments. Some of the bands seen are even stronger in the A-10 KO cells than in the A-10 WT cells. Since the A-10 KO cells should not express TRPV1, I would not believe that those bands belong to TRPV1, but rather to something unspecific.

Considering all the data from our western blot studies, both used antibodies seem to be rather unspecific as they seem to bind several proteins and the size of those proteins accidentally corresponds to the expected size of TRPV1.

As previously described (4.5), nondifferentiated PC-12 cells were tested with all three custom designed primers. Since a signal for the presumable TRPV1 in nondifferentiated PC-12 cells appeared

at the same cycle as those from water, RT+ and RT-, and the melting curves for all tested primers were not good, we conclude that nondifferentiated PC-12 cells do not seem to express TRPV1 mRNA. Differentiated PC-12 cells produced a nice signal with the primer set 1, suggesting that they do express TRPV1 mRNA.

Due to this data from the qPCR, we would not expect TRPV1 expression in nondifferentiated PC-12 cells, but we would expect TRPV1 expression in differentiated PC-12 cells. When observing the western blot results, we could indeed detect a double band at around 90 kDa in differentiated PC-12 cells in two out of three experiments, suggesting that this could possibly be TRPV1. This double band could neither be detected in nondifferentiated PC-12 cells, nor in A-10 and VSMC.

We could detect TRPV1 mRNA in our VSMC. Nonetheless, the signal for TRPV1 appeared at a later cycle as those for the loading control GAPDH, suggesting only a small amount of TRPV1 mRNA. In the first experiment TRPV1 mRNA was expressed in VSMC grown for 2 days and serum-deprived VSMC. Although standard deviations were high, we could observe a 2-fold increase in TRPV1 mRNA in the serum-deprived VSMC. We could also show TRPV1 mRNA expression in the second experiment, here standard deviations were not high. As in the first experiment, TRPV1 mRNA expression was much higher in the serum-deprived VSMC than in the VSMC grown for two days.

However, when observing the western blot results of VSMC, in all three experiments we detected a stronger band in VSMC grown for 2 days than in the serum-deprived VSMC. Therefore, the data from our qPCR experiments do not reflect the results from our western blot studies.

5.4. Phalloidin staining of VSMC

Phalloidin staining has previously been performed in our study group. Staining of PDGF-induced VSMC led to rearrangement of actin cytoskeleton upon 6 h evodiamine exposure. However, in this study we could not reproduce this effect. Evodiamine treatment revealed no rearrangement of the actin cytoskeleton in our experiments.

5.5. Conclusion and Outlook

In this diploma thesis, we could corroborate previous results from the "Molecular targets" group regarding the anti-proliferative effect of evodiamine and capsaicin in VSMC. This anti-proliferative effect is due to G2/M arrest of PDGF-induced VSMC after evodiamine treatment. Moreover, we identified a possible TRPV1 dependency of this effect, since TRPV1 antagonists capsazepine and SB-366791 overrode the anti-proliferative effect of evodiamine. However, this should be confirmed in gene-knockdown/knockout studies, as antagonists might exert some additional effects in cells independent from TRPV1.

We did detect TRPV1 mRNA in our VSMC model, with an increase of TRPV1 mRNA in serum-deprived VSMC compared to VSMC grown for 2 days. However, results with the western blot on TRPV1 expression in our VSMC were inconclusive. Results with both antibodies showed stronger bands with the VSMC grown for two days, therefore not corresponding with our qPCR data. Additionally, we can observe bands with both, the A-10 WT and KO cells, leading to the conclusion that the antibodies might bind in an unspecific manner. Therefore, we would not expect what we observed in our western blot studies to actually be TRPV1.

Examining the bands which we would expect to be TRPV1 using mass spectrometry would be a possible way to find out if the antibodies actually bind TRPV1 or other proteins corresponding in size.

6. Materials and Methods

6.1. Cell culture

Table 1. *Materials for cell culture.*

VSMC growth medium			
	DMEM (40%)	200 ml	Lonza Group Ltd. (Basel, Switzerland)
	HAM's F-12 (40%)	200 ml	Lonza Group Ltd. (Basel, Switzerland)
	FBS 20%	100 ml	
	Glutamine 200 mM	10 ml	
	Gentamicin sulfate amphotericin-B (GA-1000)	0.5 ml	Lonza Group Ltd. (Basel, Switzerland)
	Phenol red	1.5 ml	
VSMC starvation medium			
	DMEM	250 ml	Lonza Group Ltd. (Basel, Switzerland)
	HAM's F-12	250 ml	Lonza Group Ltd. (Basel, Switzerland)
	FBS 0.1%	0.5 ml	
	Glutamine	10 ml	
	Gentamicin sulfate amphotericin-B (GA-1000)	0.5 ml	Lonza Group Ltd. (Basel, Switzerland)
	Phenol red	1.5 ml	
	BSA 0.2%	1.0 g	
A-10 cells medium			
	DMEM	500 ml	Lonza Group Ltd. (Basel, Switzerland)
	FBS 10%	50 ml	
	Glutamine	5 ml	
PC-12 cells complete medium			
	RPMI	250 ml	Lonza Group Ltd. (Basel, Switzerland)

	FBS 5%	12.5 ml	
	Horse serum 10%	25 ml	
	Glutamine	2.5 ml	
PC-12 cells serum reduced medium			
	RPMI	250 ml	Lonza Group Ltd. (Basel, Switzerland)
	Horse serum	12.5 ml	
	Glutamine	2.5 ml	
	100 ng/ml NGF added right before use		
PBS, pH 7,4			
	NaCl	7.2 g	
	Na_2HPO_4	1.48 g	
	KH_2PO_4	0.43 g	
	dH_2O	Ad 1000 ml	
Trypsin/EDTA			
	Trypsin	0.5 g	
	NA_2-EDTA	0.2 g	
	PBS	Ad 1000 ml	

Table 2. *Substances used*

Name	**Provider**
Recombinant PDGF-BB (human)	Bachem (Weil am Rhein, Germany)
Recombinant NGF (human)	Sino Biologicals (Beijing, China)
Piperine	Sigma-Aldrich (Vienna, Austria)
Evodiamine	Sigma-Aldrich (Vienna, Austria)
(E)-Capsaicin	Bio-Techne Ltd. (United Kingdom)
Capsazepine	Bio-Techne Ltd. (United Kingdom)
SB-366791	Bio-Techne Ltd. (United Kingdom)
BCTC	Prof. Michael J. Fischer, Medical University Vienna

Table 3. *Technical equipment used*

Name	Provider
BD FACS Calibur™	BD Biosciences Pharmingen (San Diego, CA, USA)
Vi-Cell™ XR Cell Viability Analyzer	Beckman Coulter (Indianapolis, IN, USA)
Tecan Sunrise™	Tecan Group Ltd. (Männedorf, Switzerland)
LAS-3000™ Luminescent Image Analyzer	Fujifilm (Tokyo, Japan)
Inverted Microscope Olympus CKX31	Olympus Europa SE & CO. KG (Hamburg, Germany)
Confocal Microscope Leica TCS SPE	Leica Microsystems GmbH (Wetzlar, Germany)

6.2. Cultivation of VSMC

Primary vascular smooth muscle cells were usually passaged on Monday. Growth medium was removed and cells were washed with 10 ml PBS to remove serum remains. 4 ml trypsin/EDTA was then added to detach cells from the ground. After 5 min of incubation (37°C, 5% CO_2), 9 ml growth medium was added to stop trypsinization and the cell suspension was centrifuged (4 min, 410 g). The remaining pellet was re-suspended in 10 ml growth medium and cell count analyzed via Vi-Cell™. $1x10^6$ cells were then seeded on a growth area of 175 cm^2 in 20 ml growth medium.

Medium was changed every two-three days. VSMC were used between passages 8-12.

6.3. PC-12 cells

PC-12 cells (a kind gift from Prof. Harald Sitte, Medical University of Vienna) derive from a rat pheochromocytoma and differentiate in response to nerve growth factor into tumor glial cells[46]. When cultured, PC-12 cells were kept as suspension in growth medium. Upon differentiation, cells were seeded onto collagen-coated dishes and stimulated with NGF for 10-12 days in serum-reduced medium.

6.3.1. Differentiation of PC-12 cells

A 10 cm dish was coated with collagen type I. After 1 h of drying, the dish was washed 2x with PBS and left to further dry in the sterile hood for 2 h. After 2 h of drying, cells were seeded (400.000 cells/10 cm dish) and incubated (37°C, 5% CO_2).

Before removing medium of the differentiated cells, a photo was taken to document the differentiation process. Cells were then washed with serum-reduced medium and NGF in serum-reduced medium was added. This process was repeated every 2-3 days for 11 days (Figure 16).

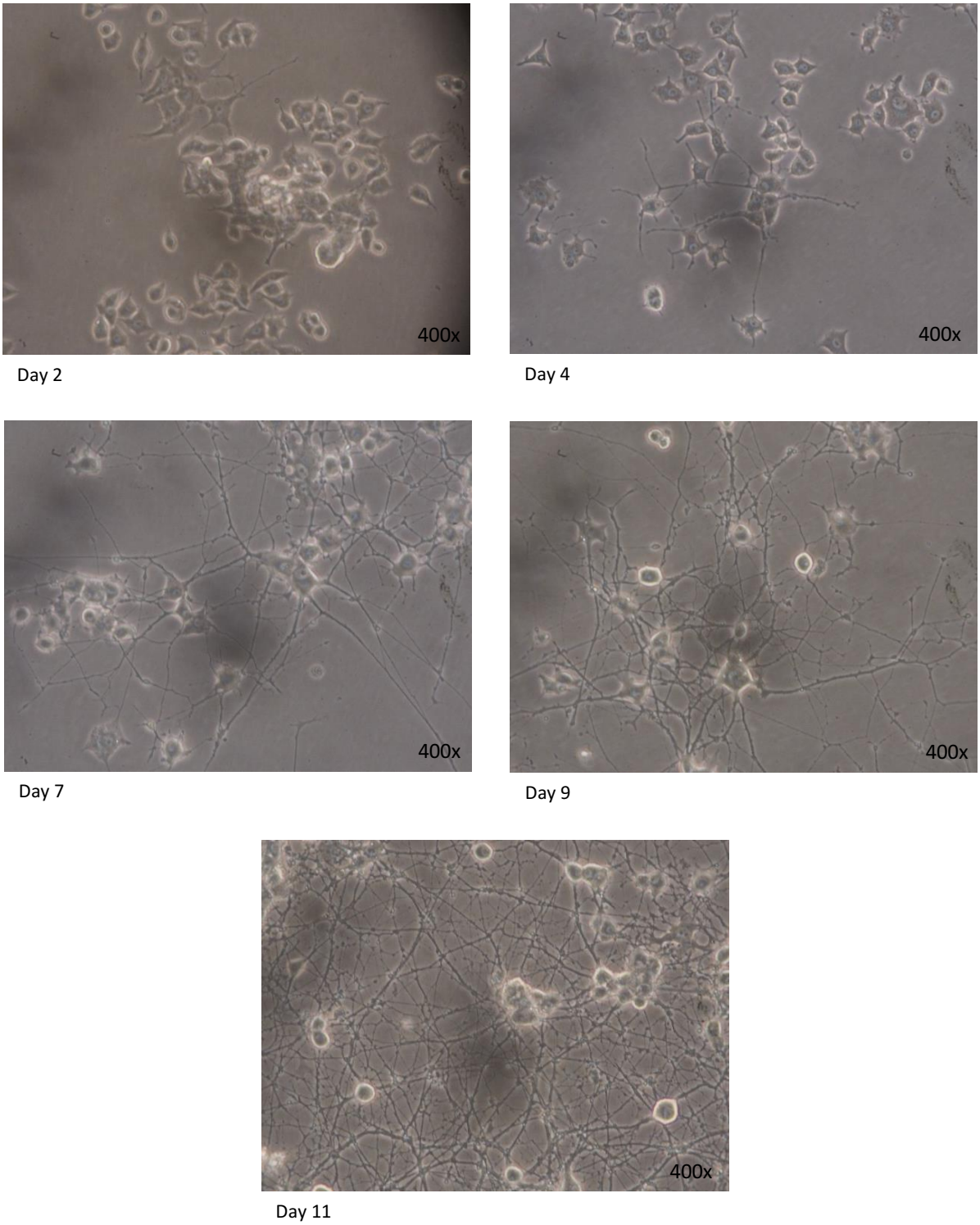

Figure 16: Differentiation of PC12 cells. *Cells were treated with 100 ng/ml NGF every 2-3 days for 11 days.*

Undifferentiated cells were seeded on a 10 cm dish (400.000 cells/10 cm dish) and grown until confluence. Both, differentiated and undifferentiated cells, were then treated with lysis buffer and prepared for western blot (6.8.1 and 6.8.2), respectively.

6.4. A-10 cells

The A-10 cell line originates from the thoracic aorta of rats and is a widely used model for vascular smooth muscle cells[47]. For this study, A-10 WT and A-10 TRPV1 KO cells were used in western blot experiments. A-10 TRPV1 KO cells were raised in the Core facility Vienna BioCenter (Vienna, Austria) through CRISPR/Cas9 method.

For experiments, cells were seeded in 6 cm dishes (400.000 cells/6 cm dish) and grown until confluent. They were then treated with lysis buffer and prepared for Western Blot (6.8.1 and 6.8.2).

6.5. LDH Assay

Lactate dehydrogenase is a common cytosolic enzyme found in all cells. Upon damage of the cell membrane, it is released into the cell culture medium. The LDH assay is based on the conversion of lactate to pyruvate in the presence of NAD^+ catalyzed by LDH (Figure 17). The reduction of INT into a red formazan salt by NADH can be measured at 490 nm[48,49,50].

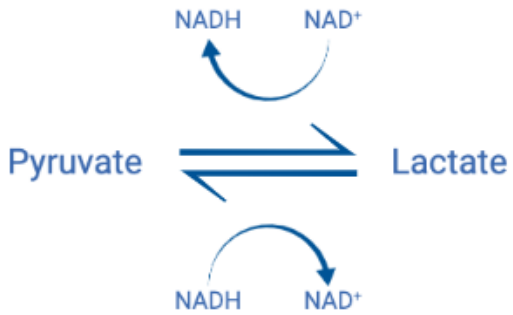

Figure 17: Reaction catalyzed by LDH. *After Valvona C.J. et al.[50]*

Vascular smooth muscle cells were seeded in a 96-well plate (10.000 cells/well) in VSMC growth medium. After 24 h growth medium was removed and cells were washed with 200 µl starvation medium. 200 µl fresh starvation medium was then added for 24 h.

After 24 h 100 µl fresh starvation medium was added to each well. Following one hour of incubation, cells were treated with 80 µl compounds or vehicle diluted in starvation medium for 30 min and then stimulated with PDGF for 24 h.

Released LDH: 100 µl of the supernatant were transferred into a new plate. Each well was treated with 20 µl lactate solution and 40 µl INT/NAD+ solution. Following 30 min of incubation, 20 µl stop solution was added and the absorbance measured at 490 nm.

Total LDH: 20 µl lysis solution was added to the rest of the supernatant in each well. Cells were then incubated at room temperature (RT) for 45 min. After adding 20 µl lactate solution and 40 µl INT/NAD+ solution, cells were incubated for 30 min. Finally, 20 µl stop solution was added to each well and the absorbance measured at 490 nm.

Table 4. *Materials for LDH Assay.*

Lactate solution		
	Lactate	36 mg/ml
	in Tris Cl 10 mM, pH 8.5	
Lysis solution		
	10% Triton-X in H_2O	
INT/NAD^+ solution		
	NAD^+	2.25 mM (1.5 mg/ml)
	Diaphorase	6.75 U/ml
	BSA	0.015%
	Sucrose	0.6%
	INT	2 mM (1 mg/ml)
	Everything dissolved in PBS, pH 8.5	
Stop solution		
	Oxamic acid	16 mg/ml
	in PBS, pH 8.5	

6.6. PI Staining

Depending on which cell cycle phase cells are in, they show different amounts of DNA. During the S phase the DNA is doubled, meaning cells in the G2/M phase have twice as much DNA than cells in the G0/G1 phase.

The DNA of VSMC was stained with propidium iodide, a fluorescent colorant. PI is not able to permeate cell membranes of viable cells, hence only the DNA of dead cells is dyed. When exposed to hypotonic fluorochrome solution (HFS), cell membranes become permeable and allow PI to bind the DNA of cells. Increase in the DNA amount is visible as the shift in the fluorescence intensity in the histogram plot when cells are being analyzed by flow cytometer.

VSMC were seeded in 6-well plates (150.000 cells/well) in 2 ml growth medium and incubated for 24 h (37°C, 5% CO_2). Growth medium was removed, cells were washed with 2 ml/well PBS and 2 ml/well starvation medium was added. Following 24 h of incubation, cells were treated with compounds or vehicle for 30 min and then stimulated with PDGF for 16 h and 24 h.

Supernatant from each well was transferred into a cytometry tube. Cells were washed with 1000 µl/well PBS, which was then also moved into the cytometry tube. 100 µl/well trypsin/EDTA was added to detach cells from the ground. After 3 min of incubation (37°C, 5% CO_2), 900 µl/well growth medium was added to stop trypsinization and the solution transferred into the cytometry tube. Following centrifugation of the tubes (4 min, 410 g), supernatant was moved to waste and 500 µl PBS added to each cytometry tube. The tubes were centrifuged again (4 min, 410 g), supernatant moved to waste and 250 µl PI solution added to each tube. The tubes were vortexed and stored at 4°C over night.

Flow cytometry was performed using BD FACS Calibur™ (FL-2 channel).

Table 5. *Materials for flow cytometry.*

FACS buffer, pH 7.37		
	NaCl	40.6 g
	KH_2PO_4	1.3 g
	Ka_2HPO^4	11.75 g
	KCl	1.4 g
	LiCl	2.15 g
	NaN_3 (Na-Acid)	1.0 g
	Na_2EDTA	1.8 g
	ddH_2O	5000 ml
HFS		
	Triton X-100	1 g
	Sodium Citrate	1 g
	PBS	1000 ml
Propidium iodide solution (1:40)		
	Propidium iodide (2 mg/ml)	0.15 ml
	HFS	5.85 ml

6.7. Trypan blue exclusion

Trypan blue is a dye which is not able to permeate cell membranes, therefore only staining late apoptotic and necrotic cells. Using a hemocytometer (Vi-Cell™), the amount of dead and viable cells can be easily determined[51,52].

VSMC were seeded in 6-well plates (150.000 cells/well) in 2 ml growth medium and incubated for 24 h (37°C, 5% CO_2). Growth medium was removed, cells were washed with 2 ml/well PBS and 2 ml/well starvation medium was added. Following 24 h of incubation, cells were treated with compounds or vehicle for 30 min and then stimulated with PDGF for 16 h and 24 h.

To collect both the attached and the detached cells, supernatant from each well was transferred into a falcon. Cells were washed with 1000 µl/well PBS, which was then also moved into the falcon. 100 µl/well trypsin/EDTA was added to detach cells from the ground. After 3 min of incubation (37°C,

5% CO_2), 900 µl/well growth medium was added to stop trypsinization and the solution transferred into the falcon.

700 µl of each sample was transferred into a Vi-Cell™ sample vial for cell counting via Vi-Cell™. Vi-Cell™ absorbs the sample which is then mixed with trypan blue. As mentioned above, trypan blue is solely able to penetrate permeable cell membranes. Via Vi-Cell™, cells which incorporated trypan blue, like apoptotic cells, appear darker than living cells which did not incorporate trypan blue. The software uses the measurement of contrast to analyze the viability of the cells.

Vi-Cell™ results show the amount of total cells/ml and viable cells/ml. For our results, these data were normalized to 4 ml total volume and compared to the DMSO PDGF control.

6.8. SDS-PAGE and Western Blot

6.8.1. Protein extraction

Cells were seeded in 6 cm dishes (400.000 cells/dish) and incubated for 2 days until confluence. To collect cells, dishes were placed on ice and medium was removed. Cells were washed with 2 ml cold PBS and 100 µl cold lysis buffer/dish was added for 20 min. Cells were then scraped, collected in Eppendorf tubes and stored at -80°C.

For protein extraction cells were thawed and centrifuged for 20 min (4°C, 21.100 g) to remove insoluble membranes. Supernatant was moved into a new Eppendorf tube with 3xSDS buffer (1:3). Proteins were cooked at 96°C for 10 min and then stored at -20°C until used for Western Blot.

Table 6. *Buffers for protein extraction*

Lysis buffer/6 cm dish		
	RIPA buffer	105 µl
	Complete	4.5 µl
	PMSF	1.1 µl
	NaF	0.6 µl
	Na_2VO_4	0.6 µl
RIPA buffer		
	Tris HCl	394.0 mg
	NaCl	438.3 mg
	Nonidet P 40	500.0 mg
	Deoxycholat	125.0 mg
	SDS	50.0 mg
3 x SDS sample buffer		
	0.5 M Tris HCl, pH 6.8	37.5 ml
	SDS	6.0 g
	Glycerol	30.0 ml
	Bromophenol blue	15.0 mg
	Aqua dest.	ad 100 ml

15% ß-Mercaptoethanol added right before use

6.8.2. Bradford assay

The dye Coomassie Brilliant Blue G-250 binds proteins and therefore is used for determining protein concentration. The higher the intensity of the Coomassie stain, the more protein the sample contains. Protein concentrations are determined for the following SDS gel electrophoresis, in order to load the same amount of protein for each pocket.

190 µl 5x Roti Quant solution 1:5 diluted with ddH_2O (Bradford reagent) was added to each well of a 96-well plate. 5 µl supernatant from the previous centrifuged samples (6.8.1) was moved into a new Eppendorf tube and diluted with 45 µl ddH2O. 10 µl from the sample solution was then added to the Bradford reagent in the 96-well plate with a total dilution factor of 1:200.

In order to be able to calculate the protein concentrations of the samples a calibration curve was used (Table 7). These serial dilutions of bovine serum albumin were mixed with Bradford reagent in the same manner as the samples were.

The absorbance of the calibration curve and the samples was measured at 595 nm in triplicate using the microplate reader Tecan Sunrise™. Protein concentrations of the samples were then calculated using the calibration curve.

Table 7. *BSA calibration curve for Bradford*

BSA end concentration (µg/ml) in Bradford reagent	**BSA end concentration (µg/ml)**	**Preparation (µl stock + H_2O)**
2.5	50	50 + 950
5	100	100 + 900
7.5	150	150 + 850
10	200	200 + 800
15	300	300 + 700
20	400	400 + 600
25	500	500 + 500

6.8.3. SDS-PAGE

SDS is an anionic detergent, which binds proteins and destroys their physiological protein folding[15]. After denaturation, proteins can be separated using electrophoresis. Proteins are loaded onto the gel and separated according to their molecular weight. Voltage application ensures faster separation of the proteins, during which smaller proteins are moving faster and large proteins need more time running through the gel[53].

40 µg protein/pocket was loaded on a 6% PAA gel in 1x epho buffer and separated via electrophoresis using a Mini-PROTEAN™ 3 cell system (BIO-RAD) (Table 8). For stacking the proteins, electrophoresis was performed at 60 V and for separating the proteins at 150 V.

Table 8. *Materials for SDS-PAGE*

Separation gel 6%		
	30% PAA	1.6 ml
	1.5 M Tris HCl, pH 8.8	2 ml
	10% SDS	80 µl
	H_2O dest.	4.2 ml
	TEMED	8 µl
	10% APS	80 µl
Stacking gel		
	30% PAA	1 ml
	1.25 M Tris HCl, pH 6.8	500 µl
	10% SDS	50 µl
	H_2O bidest.	3.35 ml
	TEMED	5 µl
	10% APS	50 µl
10x Epho buffer		
	Tris Base	30 g
	Glycine	144 g
	SDS	10 g
	Aqua dest.	ad 1000 ml
1x Epho buffer		
	10x epho buffer	100 ml
	Aqua dest.	900 ml

6.8.4. Western Blot

Proteins were transferred onto a PVDF membrane using the tank blotting procedure (90 min at 0.11 A). Membranes were then blocked with 5% milk in 1x TBS-T at room temperature (RT) for 1 h. After a washing step with 1x TBS-T, membranes were incubated with the primary antibodies at 4°C overnight. After another three steps of washing with 1xTBS-T, membranes were incubated with the secondary antibodies at RT for 1 h. Following three washing steps with 1x TBS-T, detection solution

was added to the membranes and proteins detected using a LAS-3000™ image reader. Quantification of the protein bands was performed using the Multi Gauge software.

Table 9. Materials used in Western Blot analysis.

5x Blotting buffer		
	Tris base	15.169 g
	Glycine	72.9 g
	Aqua dest.	ad 1000 ml
1x Blotting buffer		
	5x blotting buffer	200 ml
	Methanol	200 ml
	Aqua dest.	600 ml
1x TBS-T		
	Tris base	3 g
	NaCl	11.1 g
	Tween 20	1 ml
	Aqua dest.	ad 1000 ml
Detection solution		
	ECL buffer	500 µl
	ddH2O	4.5 ml
	Luminol	22.5 µl
	p-Coumaric acid	11.12 µl
	30% H2O2	1.5 µl
ECL buffer		
	Aqua dest.	9000 µl
	Tris- base	1000 µl
	Luminol	50 µl
	p-Coumaric acid	22 µl
	30% H2O2	3 µl

Table 10. *Antibodies used in Western Blot analysis.*

	Target	Host	Dilution	Provider
Primary antibodies				
	Anti-VR1 antibody – C-terminal	Mouse, monoclonal	1:500 in 5% milk in 1x TBS-T	Abcam (Cambridge, MA, USA)
	Vanilloid R1/TRPV1 antibody – N-terminal	Rabbit	1:1000 in 5% milk in 1x TBS-T	Novus Biologicals
	α,β Tubulin	Rabbit, polyclonal	1:5000 in 5% BSA	Cell Signaling Technology® (Danvers, MA, USA)
Secondary antibodies				
	Anti-mouse IgG HRP linked	Horse	1:1000 in 5% milk in 1x TBS-T	Cell Signaling Technology® (Danvers, MA, USA)
	Anti-rabbit IgG HRP linked	Goat	1:2500 in 5% BSA	Cell Signaling Technology® (Danvers, MA, USA)

6.9. Real time quantitative polymerase chain reaction

6.9.1. RNA isolation

VSMC were seeded (600.000 cells/dish) in 6 cm dishes in growth medium. After 24 h of incubation, growth medium from one dish was removed and replaced with diet medium for another 24 h. Medium was then removed, cells were washed with PBS and 400 µl/dish TRK lysis buffer was added for 5 min. Cells were scraped and stored at -80°C.

RNA isolation was performed using the PeqGOLD Total RNA Kit. Thawed samples were loaded onto homogenizer columns and centrifuged (2 min, 13.500 g). Lysates were then mixed with 70% EtOH, loaded onto RNA binding columns and centrifuged (1 min, 10.000 g). After washing with 500 µl washing buffer I, columns were centrifuged again. Columns were then washed with 500 µl 80% EtOH and centrifuged. For drying, the columns were centrifuged at maximum speed for 2 min and then

transferred into a new Eppendorf tube. 40 µl RNAse free water was added, the tubes centrifuged and stored at -80°C.

6.9.2. Reverse transcription to cDNA

Reverse transcription to cDNA was performed using the Applied Biosystems™ High Capacity cDNA Reverse Transcription Kit. 1 µg RNA was diluted in 10 µl Nuclease-free H_2O and 10 µl 2X RT master mix added to the RNA samples. The tubes were centrifuged briefly and then loaded into the thermal cycler.

6.9.3. Real time quantitative PCR

The polymerase chain reaction (PCR) is a commonly used method to amplify DNA. The first step of this process is denaturation, where double stranded DNA is separated into two single strands via high temperature. Cooling down leads to attachment of the primers (synthesized by Dr. Tina Blazevic using ncbi tool, Table 12) to the DNA. Temperature is then increased again to synthesize the new DNA strand, with the help of DNA polymerase. In one cycle of PCR, DNA is doubled, therefore repeating cycles are able to generate multiple copies of the template DNA[54]. In addition, using real time qPCR provides the possibility of quantification in real time. Quantification is performed using fluorescent dyes, such as SYBR Green, or hydrolysis probes, such as TaqMan™[55]. SYBR Green is able to interact with double stranded DNA. Following complex formation, the fluorescence of SYBR Green is increased[56].

Real time qPCR was performed using the Luna® Universal qPCR Master Mix. cDNA was used undiluted for the target gene detection, whereas for the housekeeping gene (GAPDH) a 1:20 dilution was used. Total reaction volume was 15 µl and included 1.5 µl cDNA, 7.5 µl Luna Universal qPCR Master Mix, 0.75 µl primer solution and 5.25 µl nuclease-free water.

Samples were measured in triplicate.

Table 11. *Kits used for RT-qPCR.*

Name	Provider
PeqGOLD Total RNA Kit	VWR Life Science (Darmstadt, Germany)
High-Capacity cDNA Reverse Transcription Kit	Applied Biosystems (Foster City, CA, USA)
Luna® Universal qPCR Master Mix	New England Biolabs (Ipswich, MA, USA)

Table 12. *Primers used.*

Target	5' to 3' sequence	Provider
Rat TRPV1 (Primer 1)	Forward: TTCACCGAATGGGCCTATGG Reverse: TGACGGTTAGGGGTCTCACT	Invitrogen (Carlsbad, CA, USA)
Rat TRPV1 (Primer 2)	Forward: GGGTGGACGAGGTAAACTGG Reverse: TTCTCCCTGAAACTCGGCCT	Invitrogen (Carlsbad, CA, USA)
Rat TRPV1 (Primer 3)	Forward: CCTAGCTGGTTGCAAATTGGG Reverse: TGGAGGTGGCTTGCAGTTAG	Invitrogen (Carlsbad, CA, USA)

6.10. Phalloidin staining of VSMC

Sterile precision coverslips were placed in each well of a 12-well plate and covered with 0.1% gelatin solution. After 30 min incubation (37°C, 5% CO_2), the extra gelatin solution was aspirated and VSMC were seeded (50.000 cells/well) in growth medium on the cover slips. Growth medium was removed the next day and replaced with fresh diet medium. Following 24 h of incubation (37°C, 5% CO_2), cells were treated with compounds or vehicle for 30 min and then stimulated with PDGF for 6 h and 16 h.

Medium was removed, cells were washed with PBS and incubated with 500 µl/well 4% paraformaldehyde in PBS for 10 min (37°C, 5% CO_2). After the fixation, cells were washed 3x with PBS and then stored at 4°C over night.

Cells were incubated (37°C, 5% CO_2) with 500 µl/well of 0.2% Triton X-100 in PBS for 10 min and then washed 3x with 1x TBS-T. In dark, moist conditions cells were blocked in 10% goat serum in 1x TBS-T for 1 h at room temperature (RT). After blocking, coverslips were washed 3x with 1x TBS-T and then incubated with 20 µl of DyLight™ 488 Phalloidin for 15 min at RT. Coverslips were washed 3x with 1x TBS-T and then incubated with 20 µl Hoechst dye solution for 1 min. After rinsing with PBS, the coverslips were placed on a preparation glass with a drop of mounting medium and stored at 4°C over night (Table 13).

Samples were observed under the confocal microscope (Leica TCS SPE, Leica Microsystems GmbH, Wetzlar, Germany).

Table 13. *Materials used for Immunostaining.*

Name	**Provider**
DyLight™ 488 Phalloidin, dilution 1:40 in 1xTBS-T	Cell Signaling Technology® (Danvers, MA, USA)
Hoechst dye 1 µg/ml in PBS	
Fluoromount™ Aqueous Mounting Medium	Sigma-Aldrich (Vienna, Austria)

6.11. Statistics

Unless stated otherwise, one-way ANOVA test was used for performance of statistical analysis (GraphPad PRISM software).

7. References

1. Lusis, A. J. Atherosclerosis. *Nature* **407**, 233–241 (2000).

2. Rudijanto, A. The role of vascular smooth muscle cells on the pathogenesis of atherosclerosis. *Acta Medica Indones.* **39**, 86–93 (2007).

3. Dzau, V. J., Braun-Dullaeus, R. C. & Sedding, D. G. Vascular proliferation and atherosclerosis: New perspectives and therapeutic strategies. *Nat. Med.* **8**, 1249–1256 (2002).

4. Silbernagl, S. & Lang, F. *Taschenatlas der Pathophysiologie*. (Thieme, 2005).

5. *Pharmakotherapie: klinische Pharmakologie: [das Lehrbuch zum Querschnittsfach]*. (Springer, 2010).

6. Zargham, R. Preventing restenosis after angioplasty: a multistage approach. *Clin. Sci.* **114**, 257–264 (2008).

7. Toklu, B. & Bangalore, S. Choosing the right coronary stent in the modern era. *Curr. Cardiol. Rep.* **16**, 469 (2014).

8. Pleva, L., Kukla, P. & Hlinomaz, O. Treatment of coronary in-stent restenosis: a systematic review. *J. Geriatr. Cardiol. JGC* **15**, 173–184 (2018).

9. Cortese, B. *et al.* Drug-coated balloon treatment of coronary artery disease: A position paper of the Italian Society of Interventional Cardiology. *Catheter. Cardiovasc. Interv.* **83**, 427–435 (2014).

10. Marx, S. O., Totary-Jain, H. & Marks, A. R. Vascular smooth muscle cell proliferation in restenosis. *Circ. Cardiovasc. Interv.* **4**, 104–111 (2011).

11. Kumar, V., Abbas, A. K. & Fausto, N. *Robbins and Cotran pathologic basis of disease*. (Saunders, 2005).

12. Basatemur, G. L., Jørgensen, H. F., Clarke, M. C. H., Bennett, M. R. & Mallat, Z. Vascular smooth muscle cells in atherosclerosis. *Nat. Rev. Cardiol.* **16**, 727–744 (2019).

13. Frismantiene, A., Philippova, M., Erne, P. & Resink, T. J. Smooth muscle cell-driven vascular diseases and molecular mechanisms of VSMC plasticity. *Cell. Signal.* **52**, 48–64 (2018).

14. Tessema, M., Lehmann, U. & Kreipe, H. Cell cycle and no end. *Virchows Arch.* **444**, 313–323 (2004).

15. W. Müller-Esterl. *Biochemie*. (Springer Spektrum, 2018).

16. Heuvel, S. van den. *Cell-cycle regulation*. *WormBook: The Online Review of C. elegans Biology [Internet]* (WormBook, 2005).

17. Johnson, D. G. & Walker, C. L. Cyclins and cell cycle checkpoints. *Annu. Rev. Pharmacol. Toxicol.* **39**, 295–312 (1999).

18. Lents, N. H. & Baldassare, J. J. Cyclins and Cyclin-Dependent Kinases. in *Encyclopedia of Cell Biology* (eds. Bradshaw, R. A. & Stahl, P. D.) 423–431 (Academic Press, 2016). doi:10.1016/B978-0-12-394447-4.30057-8.

19. Duronio, R. J. & Xiong, Y. Signaling Pathways that Control Cell Proliferation. *Cold Spring Harb. Perspect. Biol.* **5**, (2013).

20. Moran, M. M. TRP Channels as Potential Drug Targets. *Annu. Rev. Pharmacol. Toxicol.* **58**, 309–330 (2018).

21. Samanta, A., Hughes, T. E. T. & Moiseenkova-Bell, V. Y. Transient Receptor Potential (TRP) Channels. *Subcell. Biochem.* **87**, 141–165 (2018).

22. Zhang, X., Hu, M., Yang, Y. & Xu, H. Organellar TRP channels. *Nat. Struct. Mol. Biol.* **25**, 1009–1018 (2018).

23. Tóth, A. *et al.* Vanilloid receptor-1 (TRPV1) expression and function in the vasculature of the rat. *J. Histochem. Cytochem. Off. J. Histochem. Soc.* **62**, 129–144 (2014).

24. Phan, T. X. *et al.* TRPV1 expressed throughout the arterial circulation regulates vasoconstriction and blood pressure. *J. Physiol.* **598**, 5639–5659 (2020).

25. Iwaoka, E. *et al.* Evodiamine suppresses capsaicin-induced thermal hyperalgesia through activation and subsequent desensitization of the transient receptor potential V1 channels. *J. Nat. Med.* **70**, 1–7 (2016).

26. Pearce, L. V. *et al.* Evodiamine functions as an agonist for the vanilloid receptor TRPV1. *Org. Biomol. Chem.* **2**, 2281–2286 (2004).

27. Meghwal, M. & Goswami, T. K. Piper nigrum and Piperine: An Update. *Phytother. Res.* **27**, 1121–1130 (2013).

28. Lee, K. P., Lee, K., Park, W.-H., Kim, H. & Hong, H. Piperine Inhibits Platelet-Derived Growth Factor-BB-Induced Proliferation and Migration in Vascular Smooth Muscle Cells. *J. Med. Food* **18**, 208–215 (2014).

29. Sharma, S. K., Vij, A. S. & Sharma, M. Mechanisms and clinical uses of capsaicin. *Eur. J. Pharmacol.* **720**, 55–62 (2013).

30. Evangelista, S. Novel therapeutics in the field of capsaicin and pain. *Expert Rev. Clin. Pharmacol.* **8**, 373–375 (2015).

31. Douat, J., Vachon, P. & Beaudry, F. Characterization of in vitro metabolism of capsazepine, a vanilloid transient receptor potential channel antagonist, by liquid chromatography quadrupole ion trap mass spectrometry. *Biomed. Chromatogr.* **25**, 479–492 (2011).

32. Bevan, S. *et al.* Capsazepine: a competitive antagonist of the sensory neurone excitant capsaicin. *Br. J. Pharmacol.* **107**, 544–552 (1992).

33. Benko, R. *et al.* Use and limitations of three TRPV-1 receptor antagonists on smooth muscles of animals and man: a vote for BCTC. *Eur. J. Pharmacol.* **674**, 44–50 (2012).

34. Vennekens, R., Owsianik, G. & Nilius, B. Vanilloid transient receptor potential cation channels: an overview. *Curr. Pharm. Des.* **14**, 18–31 (2008).

35. Niiyama, Y., Kawamata, T., Yamamoto, J., Furuse, S. & Namiki, A. SB366791, a TRPV1 antagonist, potentiates analgesic effects of systemic morphine in a murine model of bone cancer pain †. *Br. J. Anaesth.* **102**, 251–258 (2009).

36. Gunthorpe, M. J. *et al.* Identification and characterisation of SB-366791, a potent and selective vanilloid receptor (VR1/TRPV1) antagonist. *Neuropharmacology* **46**, 133–149 (2004).

37. Fredriksson, L., Li, H. & Eriksson, U. The PDGF family: four gene products form five dimeric isoforms. *Cytokine Growth Factor Rev.* **15**, 197–204 (2004).

38. Ricci, C. & Ferri, N. Naturally occurring PDGF receptor inhibitors with potential anti-atherosclerotic properties. *Vascul. Pharmacol.* **70**, 1–7 (2015).

39. Yang, X.-P., Pei, Z.-H. & Ren, J. Making up or breaking up: the tortuous role of platelet-derived growth factor in vascular ageing. *Clin. Exp. Pharmacol. Physiol.* **36**, 739–747 (2009).

40. Andrae, J., Gallini, R. & Betsholtz, C. Role of platelet-derived growth factors in physiology and medicine. *Genes Dev.* **22**, 1276–1312 (2008).

41. Meens, M. J. P. M. T., Pfenniger, A. & Kwak, B. R. Risky communication in atherosclerosis and thrombus formation. *Swiss Med. Wkly.* **142**, w13553 (2012).

42. van Tonder, A., Joubert, A. M. & Cromarty, A. D. Limitations of the 3-(4,5-dimethylthiazol-2-yl)-2,5-diphenyl-2H-tetrazolium bromide (MTT) assay when compared to three commonly used cell enumeration assays. *BMC Res. Notes* **8**, (2015).

43. Gonzalez, R. J. & Tarloff, J. B. Evaluation of hepatic subcellular fractions for Alamar blue and MTT reductase activity. *Toxicol. In Vitro* **15**, 257–259 (2001).

44. Vega, E. & Pugsley, M. An overview of colorimetric assay methods used to assess survival or proliferation of mammalian cells. *Proc. West. Pharmacol. Soc.* **54**, 10–4 (2011).

45. Amantini, C. *et al.* Triggering of transient receptor potential vanilloid type 1 (TRPV1) by capsaicin induces Fas/CD95-mediated apoptosis of urothelial cancer cells in an ATM-dependent manner. *Carcinogenesis* **30**, 1320–1329 (2009).

46. Das, K. P., Freudenrich, T. M. & Mundy, W. R. Assessment of PC12 cell differentiation and neurite growth: a comparison of morphological and neurochemical measures. *Neurotoxicol. Teratol.* **26**, 397–406 (2004).

47. Rao, R. S., Miano, J. M., Olson, E. N. & Seidel, C. L. The A10 cell line: a model for neonatal, neointimal, or differentiated vascular smooth muscle cells? *Cardiovasc. Res.* **36**, 118–126 (1997).

48. Sepp, A., Binns, R. M. & Lechler, R. I. Improved protocol for colorimetric detection of complement-mediated cytotoxicity based on the measurement of cytoplasmic lactate dehydrogenase activity. *J. Immunol. Methods* **196**, 175–180 (1996).

49. Fotakis, G. & Timbrell, J. A. In vitro cytotoxicity assays: comparison of LDH, neutral red, MTT and protein assay in hepatoma cell lines following exposure to cadmium chloride. *Toxicol. Lett.* **160**, 171–177 (2006).

50. Valvona, C. J., Fillmore, H. L., Nunn, P. B. & Pilkington, G. J. The Regulation and Function of Lactate Dehydrogenase A: Therapeutic Potential in Brain Tumor. *Brain Pathol. Zurich Switz.* **26**, 3–17 (2016).

51. Strober, W. Trypan blue exclusion test of cell viability. *Curr. Protoc. Immunol.* **Appendix 3**, Appendix 3B (2001).

52. Crowley, L. C., Marfell, B. J., Christensen, M. E. & Waterhouse, N. J. Measuring Cell Death by Trypan Blue Uptake and Light Microscopy. *Cold Spring Harb. Protoc.* **2016**, (2016).

53. Luttmann, W., Bratke, K., Küpper, M. & Myrtek, D. *Der Experimentator: Immunologie*. (Springer Spektrum, 2014).

54. Mülhardt, C. *Der Experimentator: Molekularbiologie/ Genomics*. (Spektrum Akademischer Verlag, 2009).

55. Holzapfel, B. & Wickert, L. Die quantitative Real-Time-PCR (qRT-PCR). Methoden und Anwendungsgebiete. *Biol. Unserer Zeit* **37**, 120–126 (2007).

56. Dragan, A. I. *et al.* SYBR Green I: Fluorescence Properties and Interaction with DNA. *J. Fluoresc.* **22**, 1189–1199 (2012).

Ich habe mich bemüht, sämtliche Inhaber der Bildrechte ausfindig zu machen und ihre Zustimmung zur Verwendung der Bilder in dieser Arbeit eingeholt. Sollte dennoch eine Urheberrechtsverletzung bekannt werden, ersuche ich um Meldung bei mir.

Acknowledgements

First of all, I would like to thank Univ.-Prof. Dr. Verena Dirsch for the possibility of writing my diploma thesis at the Department of Pharmaceutical Sciences, Division of Pharmacognosy with the Molecular Targets Group.

I would also like to thank Dr. Tina Blazevic, who took the time and showed me everything in detail and supported me throughout my entire work.

Thanks to the whole Molecular Targets group for having me and always helping me when needed.

My special thanks go to my parents, who always encouraged me and supported me in every way possible. I could not have done it without them.